

Asymmetric Influence of Employees and Trading Partners on Company's Sales and its Dynamical Origin

Yuh Kobayashi*

*Department of Mathematical and Computing Science, School of Computing,
Tokyo Institute of Technology, Yokohama 226-8502, Japan*

Hideki Takayasu†

Sony Computer Science Laboratories, Tokyo 141-0022, Japan

Shlomo Havlin‡

Department of Physics, Bar-Ilan University, Ramat-Gan 52900, Israel

Misako Takayasu‡

Institute of Innovative Research, Tokyo Institute of Technology, Yokohama 226-8502, Japan

(Dated: February 6, 2022)

Growth of business firms or companies has been a subject of intensive research over a century. However, there still remains controversy about the basic mechanisms of their growth. Inspired by previous work on scaling laws in other systems, here we extend the notion of size of firms from a scalar to a vector in order to characterize in more detail the mechanisms of growth and decay of firms. Based on a large scale dataset of Japanese firms covering over two million firms for two decades (1994–2015), we compile the dataset of vectors of three components, namely, annual sales, number of employee and number of trading partners. We find that the number of employees is more influential in determining firm sales compared to the number of trading partners. This asymmetry is validated by regressions of sales against these parameters and the analysis of growth rate correlations. We then explore multi-variate dynamics of firms by elaborating an evolutionary flow diagram of the averaged motion in the three-dimensional vector space. The flow diagram indicates that firms which deviate from the balanced scaling relation tend to return to this relation. We also find that firms with a chance of large sales growth suffer the risk of high disappearance rate. These results could serve for prediction and modeling of firms, and are relevant for theoretical understanding of the general principles governing complex systems.

PACS numbers: 02.50.Sk, 89.65.Gh, 89.75.Da

I. INTRODUCTION

Growth of business firms is not only an important issue for business people but it has been attracting attention of academic researchers for more than a century[1–5]. The origin of models of firm growth dates back to the Gibrat's model[2] which is based on an over-simplified assumption that a firm's growth rate is random and independent of any quantity, even of its own size[5, 6]. Recently, analyses of big datasets have shown ubiquity of the fat-tailed distributions of firm growth rates[6–9], whose distribution width depends on their sizes[6, 7, 10–12]. Correspondingly, the rates of firm disappearance show negative dependence on the firm sizes[12]. Theories have highlighted mechanisms or factors as diverse as hierarchical organization[13], stochasticity in competition[14, 15],

financial[16] or hiring/firing[17] behaviors, preferential attachment of firm 'units'[8, 18], social networks[19] and multiple independent components in firms[11, 20–22], to explain those empirical facts on size and growth. However, assumptions behind the theoretical models and their implications are rarely tested using empirical data, and this yields difficulties in reaching consensus on appropriate theoretical frameworks.

We propose here that elusiveness of the nature of firm growth comes from the fact that size of a firm is not a simple scalar quantity, as usually assumed, but it has at least three components; (i) monetary size scaled typically by the annual sales, (ii) labor size measured by the number of employee, and (iii) transaction activity size which can be characterized by the number of direct trading firms. These three quantities are mutually dependent[23, 24] and have been found to follow non-trivial scaling relations represented by power laws of the form[25, 26], $y \propto x^a$, which is a typical functional form found in general complex systems, such as animal bodies[27–31], ecological communities[32, 33], and cities[34–36]. For instance, the value of exponent a in the scaling of metabolic rate on body mass have been determined to be very close to $3/4$ in mammals[27, 29, 31] and theoretically related to the minimization of energy

* Author Email yuh.kob.2010@gmail.com; kobayashi.y.bz@m.titech.ac.jp

† Also at Institute of Innovative Research, Tokyo Institute of Technology, Yokohama 226-8502, Japan.

‡ Corresponding Author Email takayasu.m.aa@m.titech.ac.jp; Also at Department of Mathematical and Computing Science, School of Computing, Tokyo Institute of Technology, Yokohama 226-8502, Japan.

consumption in blood pumping[37]. Theoretical considerations, in turn, were able to predict dozens of other scaling exponents in natural systems of animal bodies successfully. Similarly, the unique value of $a = 2$ for humans as compared to $a = 3$ for other animals in the scaling of body mass against body length was theoretically accounted for by human bipedalism[38]. In this manner, studies of scaling relations could serve as the very basis for a deep understanding of the system’s underlying principles. However, our knowledge about scaling relations in other systems including business firms are still very limited. As for the firms system, the questions about multi-variate relationships which reflect the specific mechanisms or factors of firm growth, as well as their dynamical stability through economic changes, are still not settled.

Here we focus our study on the multi-variable relations among these three quantities of firms to clarify their growth mechanisms and their stability by analyzing a comprehensive dataset of about 2 million Japanese firms accumulated over more than 20 years since 1994. In the general framework which we apply to the firm system here, we also draw an explicit analogy between the animal body and firm: we compare annual sales to metabolic rate as it is the rate of activity in terms of money instead of energy, and the number of employees and trading partners to the animal body size. Our results represent the following two major findings.

1: When considering annual sales as a function of both number of employees and number of trading partners, the scaling exponent of employee is found to be significantly higher than that of trading partners. This implies that increasing number of employees affects more strongly the sales growth than the increase of number of trading partners. This fact is directly supported by comparing distributions of sales growth rates under the conditions that either of employee or trading partners is increased within a certain ratio range while the other is kept nearly constant.

2: In the evolutionary flow diagram, we find that firms tend to move back towards the average sales depending on their size. This indicates that the scaling relations would be recovered after perturbation. In fact, the average growth rate of sales is less than a unit for a firm with more sales compared to the ‘average firm’ of the same sizes of employees and trading partners, while otherwise the sales growth is more than a unit. As a result, in order to increase the chance of a large positive growth, a firm should try to deviate from the scaling relations by increasing either (or both) of employee or trading partners. We also find that there are some regions outside the scaling line where disappearance rates of firms are significantly higher. Therefore, a firm must often take an increasing lethal risk to make a positive growth more probable.

In summary, we first show that on average sales are affected more by increasing employees compared to increasing trading partners, and next we find that firms

on average move towards the surface of predicted sales as a function of the numbers of employees and trading partners. Additionally we observe a mild variation of the scaling exponents in the period of 1994–2015, which seem to be correlated to GDP variation. It is noteworthy that despite the variation of the scaling exponents, statistical properties of distributions around the multi-variate scaling relation are stationary throughout the whole observed period. Our finding of asymmetric multi-variate scaling and evolutionary flow diagram in a vector space can provide a more lucid and better understanding of mechanisms of firm growth. This multi-variate approach might also be relevant for better understanding the growth of complex systems in general.

II. RESULTS

A. Data Compilation

We compile the data used here from an exhaustive dataset that summarizes the description of firms by a major credit reporter in the period of 1994 to 2015 (COSMOS 2 by Teikoku Databank, Ltd.) available to us in January, 2017. The dataset contains total of 2.415×10^6 firms (1.263×10^6 in yearly average), and the number of listed firms is increasing with time (Supplementary Text 1, Supplementary Fig. S1). We filtered out a small fraction of financial firms or governmental organizations whose sales are defined very differently from other ordinary firms. We also removed a very small number of sales data which were recorded more than 8 years after the publication of the financial statement. Additionally, we excluded the sales data where the end of fiscal year changes, because some of them are not annual sales. Therefore, our final dataset, consists of totally 2.395×10^6 firms (1.247×10^6 in yearly average), primarily concerns manufacturing, construction or wholesale companies. Here, we have the data of annual sales s , which is the analogue of metabolic rate in animal bodies, and the number of employees, ℓ , which could be analogous to the animal’s cell count, as well as the data of firms’ birth and death.

We construct from the data, a trading network for every year from the list of trading relationships between firms, to obtain the degree k (i.e. the number of trading partners) of every firm. The network includes 3.051×10^6 trading links per year on average (see Supplementary Text 1 for detail). This enables us to consider the transaction size of firms in the network of trading partnership[26].

We begin by studying the open question of different power law exponents in the conditional and marginal sales distributions, which has not been addressed or mentioned anywhere else to the best of our knowledge. This leads us to the finding of asymmetric role of different aspects of firm body sizes, namely employees, ℓ , and trading partners, k , on the firm sales, s .

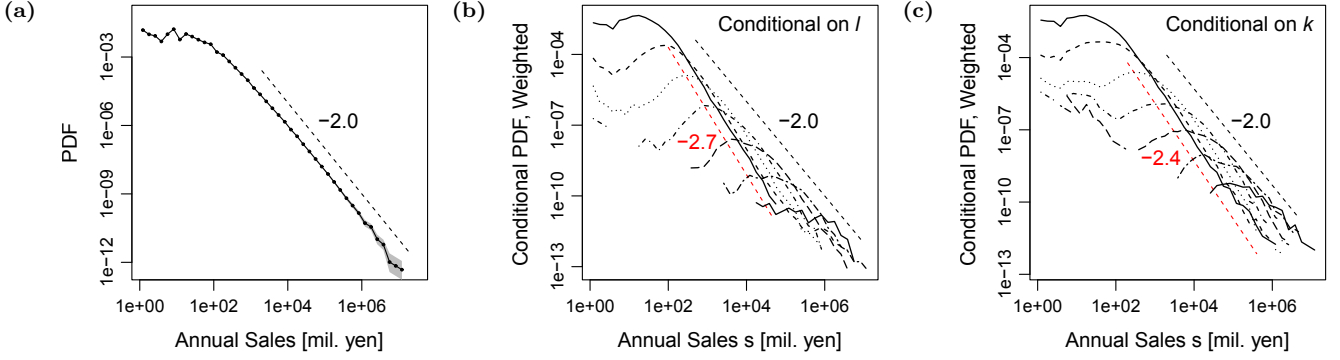


FIG. 1: Apparent inconsistency of the power-law tail exponents for marginal and conditional probability distribution functions (PDF), with an intuitive understanding based on the Bayes' theorem. (a) The probability distribution (PDF) of annual sales, plotted in log-log scales, shows a clear exponent of 2. Grey bandwidth indicates 95% confidence intervals with the assumption of Poisson process. (b–c) The conditional probability distributions $P(s|\ell)$ and $P(s|k)$, weighted with $P(\ell)$ and $P(k)$ (see Eq. (1)), plotted in log-log scales. The entire range of k and ℓ is divided into 8 levels corresponding to 8 curves, so that each interval has an identical range in the logarithmic scale. The weight of an interval is defined as the average probability density in the interval.

B. Explanation of Puzzling Scaling Exponents

It is well established that the distribution of annual sales s of firms roughly follows the Zipf's law[39, 40], that is, the probability density tail follows a power law, $P(s) \propto s^{-2}$. This is also seen in our data (see Supplementary Fig. S2c). However, when we look at the conditional sales distributions[26], the power law exponents increase to about 2.4 (for the number of trading partners k —see Fig. 1c) and about 2.7 (for employee number ℓ —see Fig. 1b) and are clearly different from 2.0 (Fig. 1a and Supplementary Figs. S4e and S4f). This seemingly contradicting results can be understood by using the Bayes' theorem as follows. Taking the case of the number of employees ℓ and annual sales s , we can approximate the integral by the contribution of the maximum values of $P(s|\ell)P(\ell)$:

$$P(s) = \int_{\ell} P(s|\ell)P(\ell)d\ell \sim P(s|\ell_{\text{lead}})P(\ell_{\text{lead}})\Delta\ell_{\text{lead}}, \quad (1)$$

where $\ell_{\text{lead}} = \arg \max_{\ell} P(s|\ell)P(\ell)$, such that $P(s|\ell)P(\ell)$ is the 'leading order' contribution, and $\Delta\ell_{\text{lead}}$ is the width of ℓ at ℓ_{lead} , which is assumed to be a constant. Indeed, when we plot in Fig. 1b the functional form of $P(s|\ell)P(\ell)$ for several typical values of ℓ based on real data, it shows clearly that the envelop function of $P(s|\ell)P(\ell)$ actually follows a power-law with the exponent close to -2.0 at its tail. Similar results are obtained also for the number of trading partners, k , as shown in Fig. 1c. A more rigorous derivation is given in Supplementary Text 3. Thus, Fig. 1 strongly suggest the origin of the well-known power law exponent of -2 for sales distribution[39, 40].

Since the known scaling relations between the size variables[26], $\ell \propto k^{1.0}$, $s \propto k^{1.2}$ and $s \propto \ell^{1.2}$ (see Supplementary Texts 2 and 4) suggest symmetric roles played by k and ℓ in determining the annual sales s , it is surprising that our results in Fig. 1 suggest strong asymmetry

between the effects of k and ℓ . Indeed, in view of magnitude of errors or fluctuations around the scaling relations, the distribution of residuals is more fat-tailed when sales, s , is regressed against k rather than when it is regressed against ℓ . This difference in the tails of fluctuation distributions implies that the number of trading partners, k , is less dominant in predicting the sales value compared to the number of employees ℓ . We discuss this novel feature in more detail in the next section.

C. Multi-variate Scaling

To assess the relative contributions of the number of trading partners, k , and the employee number, ℓ , on the annual sales s , we here generalize the scaling relationship to a multi-variate relation as follows:

$$\log s = \alpha \log k + \beta \log \ell + \varepsilon_{s|k,\ell}, \quad (2)$$

$$\text{or} \quad P(s|k, \ell) = \tilde{P}_{s|k,\ell}(s/k^{\alpha}\ell^{\beta})/k^{\alpha}\ell^{\beta}, \quad (3)$$

where α and β are the scaling exponents indicating the relative effect of k and ℓ , $\varepsilon_{s|k,\ell}$ a stochastic fluctuation term of $\log s$ conditional on both k and ℓ , $P(s|k, \ell)$ is the conditional probability density dependent on both k and ℓ , and $\tilde{P}_{s|k,\ell}$ is the scaling function. This multiple regression model roughly means $s \propto k^{\alpha}\ell^{\beta}$, and was proposed but not explored nor confirmed by real data in ref. [26]. Note that Eq. (2) is equivalent to a more formal model of regression against the orthogonalized set of variables, $\log[k]$ and $\log[\ell/k^{1.0}]$. Also note that the correlation between growth rates of k and ℓ is rather weak (Supplementary Text 5, Supplementary Fig. S8). Assuming that Eq. (2) is met, it is straightforward to derive the median value as

$$\log \langle s|k, \ell \rangle_{0.5} = \alpha \log k + \beta \log \ell + \langle \varepsilon_{s|k,\ell} \rangle_{0.5}, \quad (4)$$

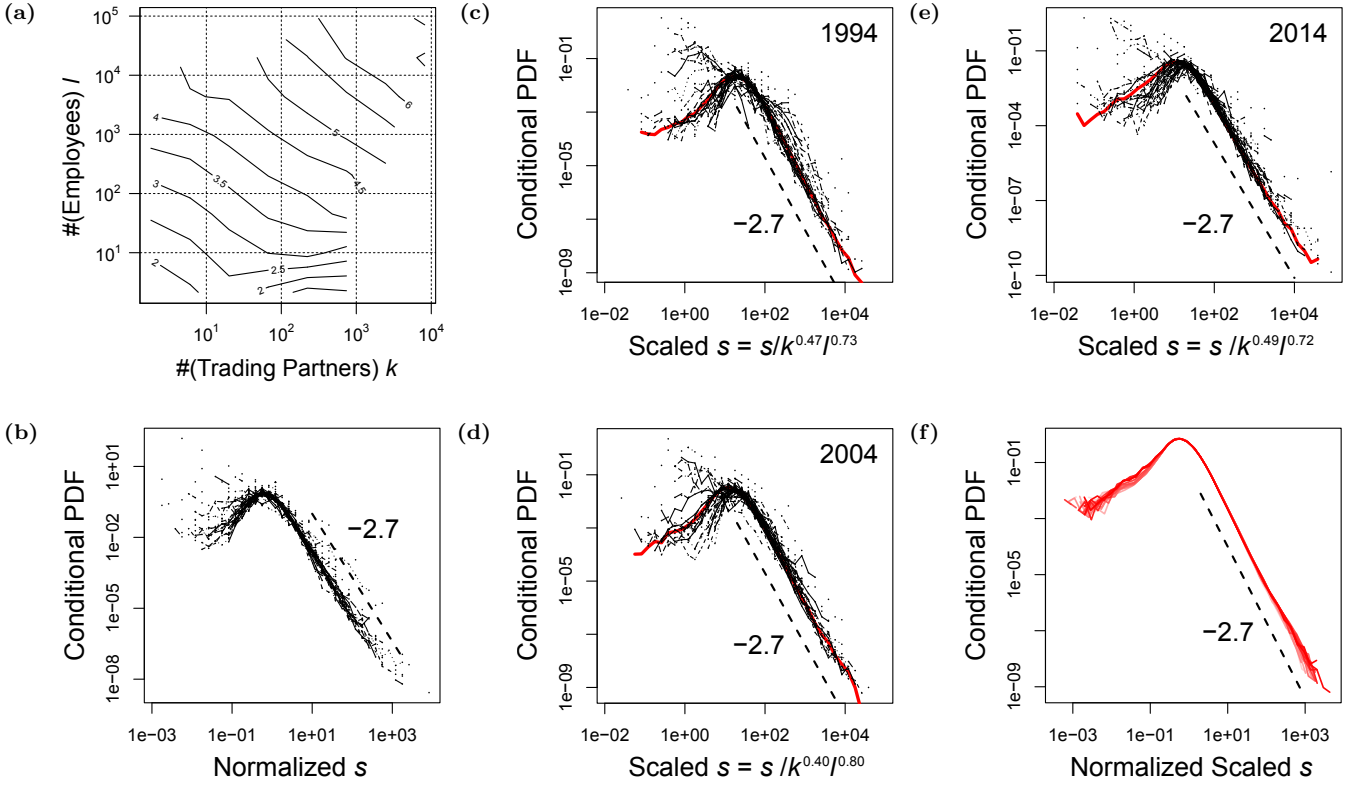


FIG. 2: Multi-variate scaling relations among the three variables. All plots are in a log-log scale. (a) Contour plot of the median values of annual sales s in million yen, conditional on both the number of trading partners k (horizontal) and the number of employees ℓ (vertical), for the 2014 data. The entire ranges of k and ℓ are divided into 8 levels, so that each interval has an identical range in log scale. The contours are obtained by linearly interpolating the log-transformed median values of sales. (b) Probability distributions (PDF) of s conditional on both k and ℓ , normalized by their medians, are plotted for the 2014 data. The conditional distributions are obtained for grids of the conditioning variables where both dimensions are divided into intervals of an identical length in log scale (2 segments per a 10-fold interval). (c–e) The probability distributions of scaled sales $s/k^\alpha \ell^\beta$ conditional on both k and ℓ , with α and β being the estimated exponents. The three panels represent results for 3 different years, namely 1994, 2004 and 2014. Red lines indicate the probability distribution of $s/k^\alpha \ell^\beta$ without any condition. The method is the same as in panel (b). (f) The probability distributions of $s/k^\alpha \ell^\beta$ for each of the 22 years (1994–2015), normalized with the medians. The exponents used are different for different years and are taken from the best values found for each year (see also Fig. 4).

where $\langle \varepsilon_{s|k,\ell} \rangle_{0.5}$ is the median value of s conditional on a specific set of k and ℓ values. If this is true, the contour plots of conditional median sales $\langle s|k,\ell \rangle_{0.5}$ on the k – ℓ logarithmic coordinate plane should show nearly regular and parallel contours. Indeed, from Fig. 2a we see that the data actually supports this expectation, especially for the medium or large values. Moreover, we find clearly that the statistical fluctuations around the median value is invariable regardless of the value of k and ℓ (Fig. 2b). This indicates that the assumption of a scaling function $\tilde{P}_{s|k,\ell}$ is valid for most of k and ℓ values. Indeed, when the distribution of scaled sales $s/k^\alpha \ell^\beta$ conditional on k and ℓ is plotted using the values of α and β estimated based on the data (Figs. 2c, 2d and 2e), we see that a remarkable fraction of the curves scale with each other. In addition, the function $\tilde{P}_{s|k,\ell}$ is surprisingly stable across years (Fig. 2f). Thus, the scaling assumptions of Eqs.

(2) and (3) are well supported by the large amount of available data.

Since $\langle \varepsilon_{s|k,\ell} \rangle_{0.5}$ in Eq. (4) is a constant, the concept of multi-variate scaling relation can be illustrated by a plane as shown in Fig. 3b. In reality, the relation is not a perfect plane, but a surface since it is curved at high- k and low- ℓ region as shown in Fig. 2a. Importantly, this marks a contrast to a ‘scaling line’ that is implied by the three scaling relationships between pairs of three variables (Fig. 3a). In fact, the bivariate scaling laws found in an earlier study[26] are naturally interpreted as projections of a single scaling line to the 2-dimensional planes, where the firms are densely distributed[41].

Our finding of $\beta > \alpha$ remains true for all years, as shown in Fig. 4, where the estimated scaling exponents for different years are plotted. For example, we have $\alpha = 0.49$ (95% confidence interval (CI) (0.455, 0.531))

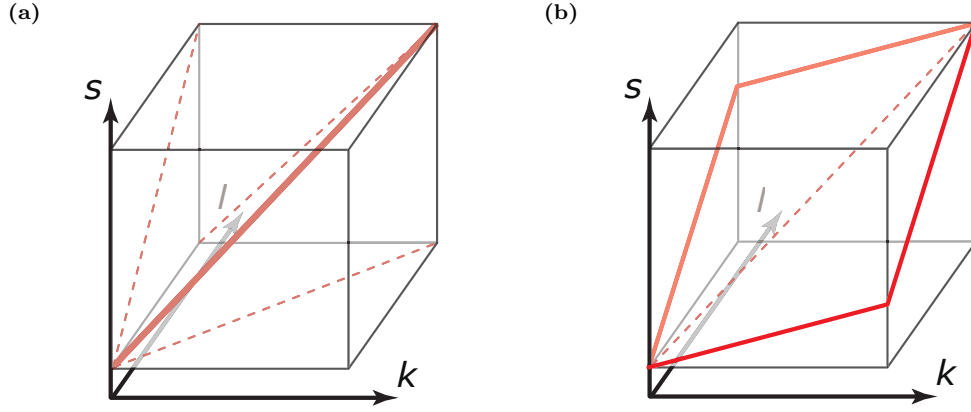


FIG. 3: Schematic illustrations of the scaling relationships. The variables k , ℓ and s respectively represent the number of trading partners, employee number and annual sales, and a firm is represented as a point in the 3-dimensional variable space. (a) Three bivariate scaling relations, indicated with the red dashed lines, can be understood as the projections of a single (red bold) ‘scaling line’. (b) The multi-variate scaling $s \propto k^\alpha \ell^\beta$ is illustrated as a plane (red solid line). The plane must include the scaling (red dashed) line, but this line clearly cannot determine a unique plane.

and $\beta = 0.72$ (95% CI (0.697, 0.744)) for 2014. Thus, we expect that the employee number ℓ actually has a larger effect on sales s compared to the number of trading partners k .

Rather unexpected is the gradual change of the values of scaling exponents that seemingly follow the economic climate. Although the inequality $\beta > \alpha$ is maintained, there is a significant change (i.e. a change beyond the CI) of α and β during the 1994–2015 period, and the changes seem almost in coherence with the nominal GDP,

as shown in Fig. 4 (bottom). Indeed, the cross correlation of estimated α and β to the nominal GDP are maximal at the time lag of one year, and as high as -0.59 for α and 0.58 for β (Supplementary Text 4; Supplementary Fig. S6c). This suggests that the exponents are strongly affected by the GDP of the preceding year. However, the exact causes of this coherence is yet to be understood.

D. Growth Correlations

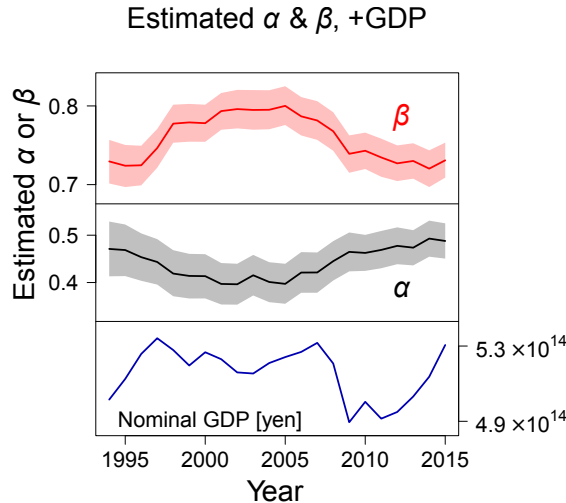


FIG. 4: Estimated exponents α (for the number of trading partners k) and β (for the number of employees ℓ) compared (in bottom plot) with the country’s nominal GDP for different years in 1994–2015. Bandwidth indicates the 95% confidence interval of the estimation obtained by the bootstrap method.

Next we test, in more detail, the asymmetry between the influence of trading partners and employees on sales. We pay attention to the firms which are on the scaling surface in one year and deviate from it in the following year, and observe their growth in annual sales. In Group 1, we include those firms that increase the number of trading partners by over a factor of 1.5 while keeping their number of employee to be $\pm 20\%$ around the original number. Similarly, in Group 2, we choose firms whose growth rate in employees is over 1.5 while their simultaneous change in the number of trading partners is within $\pm 20\%$ around their original. Fig. 5a shows the sales growth distributions for Group 1 (Black) and Group 2 (Red). The probabilities of negative sales growth is generally higher for firms with positive growth in trading partnerships, and higher sales growth is more probable for those with employee growth rather than for those with the same level of growth in trading partnerships. The mean log-transformed growth rate of sales suggests that there is an actual difference: -0.009 for firms with growth in trading partnership with 95% CI (confidence interval) of $(-0.032, 0.014)$, and 0.067 for growth in employees with 95% CI of $(0.049, 0.086)$. Consistently, two-sample Kolmogorov-Smirnov test also in-

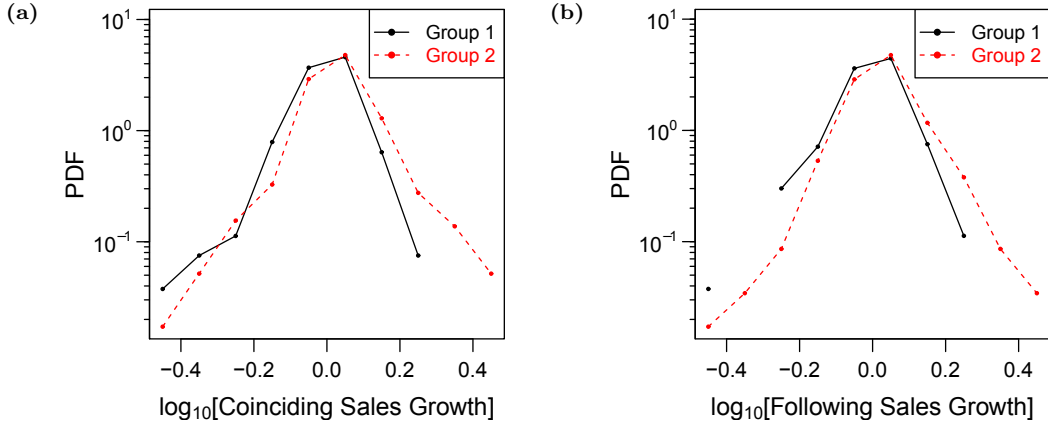


FIG. 5: Comparison of the effects of increase in trading partners and employees on sales growth. The data is aggregated for 20 years (1994–2013), and selected from around the point of scaling line for $k = 10$. The probability distributions (PDF) of log-transformed growth of annual sales, conditional on large growths of k (Group 1, black) and ℓ (Group 2, red). The conditions are $1.5 < g_k$ and $0.8 < g_\ell < 1.2$ for large k growth, and $0.8 < g_k < 1.2$ and $1.5 < g_\ell$ for large ℓ growth, where g_k and g_ℓ respectively denotes the growth rate of k and ℓ . (a) Sales growth rates at the same year as the size (employees or partners) growth. (b) Sales growth rates in the subsequent year of the size growth.

indicates that the difference is significant ($D = 0.164$, $(N_1, N_2) = (266, 581)$, $P \sim 1.2 \times 10^4$). In the following year, the difference of sales growth rate still remains clear as shown in Fig. 5b. Average log-transformed sales growth of Group 1 is 0.000 a year after with 95% CI of $(-0.027, 0.027)$, while in Group 2 it is 0.068 with 95% CI of $(0.048, 0.087)$. Also, significance is proved using two-sample Kolmogorov-Smirnov test ($D = 0.151$, $(N_1, N_2) = (266, 581)$, $P \sim 5.1 \times 10^4$). In both cases, the correlation to the sales growth is statistically significant but not strong, indicating that a rapid increase of employee number does not guarantee an immediate growth of sales but only increase the chance.

E. Evolutionary Phase Diagrams

Considering the robust scaling relations that persists throughout more than 20 years, it is natural to hypothesize that firms that are distant from the scaling surface (Figs. 2a and 3b) have the tendency of flow towards the surface. To validate this hypothesis, we elaborate ‘evolutionary flow diagrams’ by plotting the estimated vector field of annual growth in the three dimensional phase space of k , ℓ and s . This idea is inspired by previous work on the prediction of countries’ economic growth[42], where the authors advocate the applicability of Lorenz’s ‘methods of analogues’[43, 44], originally proposed for weather forecast, to economic systems. We show some slices of the vector space in Fig. 6 (also see Supplementary Fig. S9). The streamlines with arrows represent the average movement of firms parallel to the slice, while background colors indicate the average flow of firms orthogonal to the plane. The mean value of

log-transformed growth is used: for example, the mean yearly growth of sales is indicated by the average of $\log[s(t+1)/s(t)]$, where $s(t)$ is the annual sales at year t .

One can see the mean flows in sales (background colors of slices in Fig. 6) towards the scaling relation surface. Two slices of constant sales ($s = 10^{3.0}$ or $s = 10^{4.0}$ million yen, respectively) are shown in the figure. The intersection curves of the surface and slicing planes are indicated by the yellow curves. Since these contour curves indicate the firm body sizes that yield a specific value of sales for ‘average’ firms (i.e. those with median sales for their body sizes), firms in the ‘back’ of the contours in Fig. 6, located in large- ℓ regions in the slice, have less sales compared to the average firms. Sales of these firms are, therefore, below the average level. They then have positive average growth of sales represented by red background colors in Fig. 6, as hypothesized. Conversely, firms with lower ℓ below the contour curves in the constant- s slice, which have an excess of sales compared to the average, are very likely to have negative sales growth on average.

Deviations from the scaling surface are compensated not just by sales growth or decrease illustrated vertically to the slice, but also by the move along the slice, i.e. their simultaneous changes in body sizes. In fact, firms with sales disproportionate to their body sizes, which are distant from the yellow curves of scaling surface contours in Fig. 6, commonly return to the curves (Fig. 6), adjusting their body sizes to the current activity rate in sales. Note that the estimates are not so accurate at regions of large body sizes (top-right in Fig. 6) or at those with imbalanced configuration (top-left or bottom-right) as for regions of small body sizes (bottom-left), because of poor statistics due to fewer numbers of sample firms. Besides, the continuous increase of trading link data (Supplementary Text 1) is likely to add positive bias in the estimate

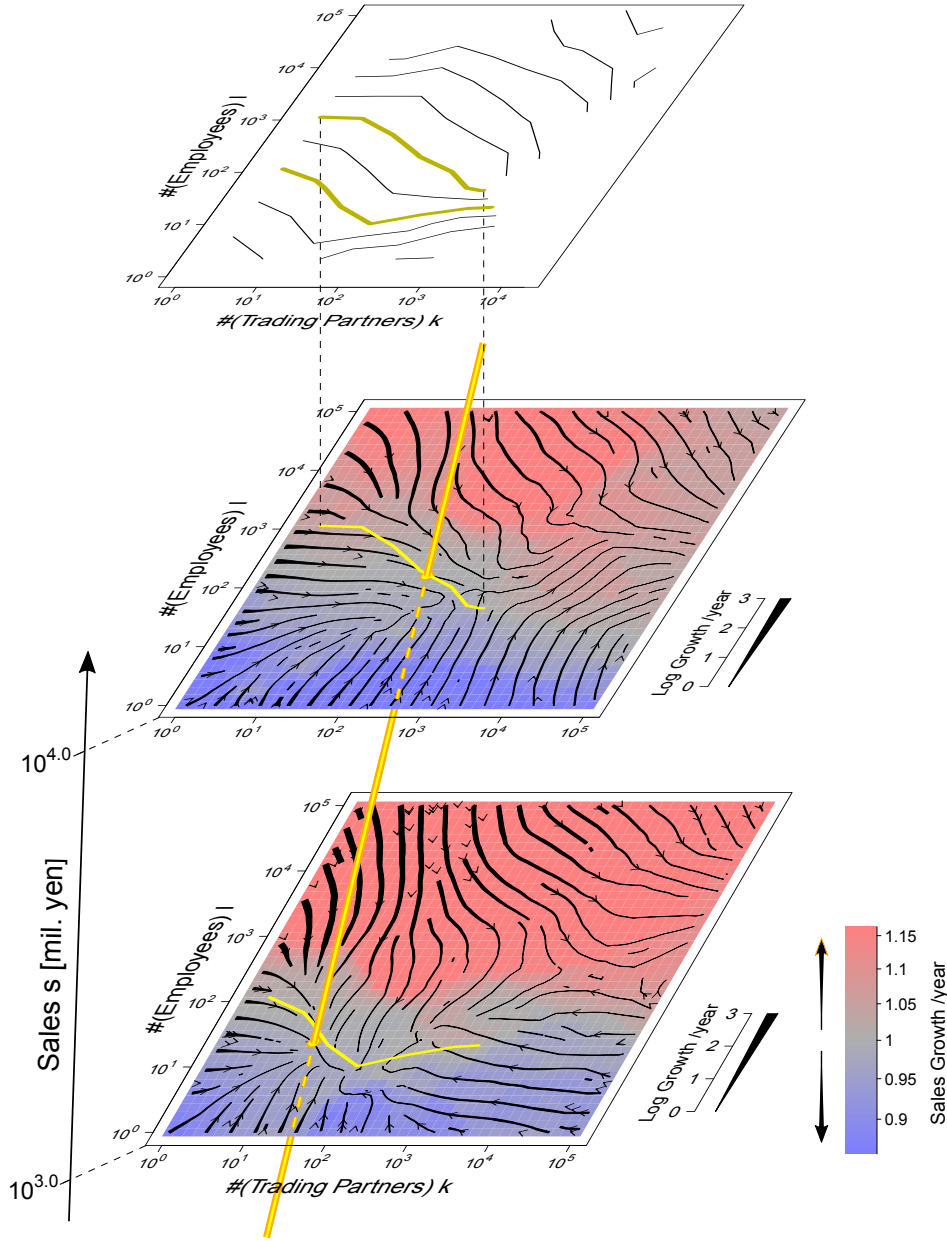


FIG. 6: Evolutionary Flow Diagram illustrating the estimated average log-transformed growth per year in slices of the vector space. The variable space is sliced by the plane of annual sales s equal to $10^{3.0}$ or $10^{4.0}$ million yen. The direction and width of the curves in the slices indicate the velocity vector of average flow within the slicing plane.

The estimated average flow orthogonal to the plane is illustrated with a background color, red, grey or blue representing plus, zero or minus sales growth, respectively. The orange and yellow line that crosses the slices represents the scaling line of bivariate relations, while yellow curves on the slices indicate the surface of multi-variate scaling, as implied by the contour plot of conditional median sales depending on the numbers of trading partners and employees, placed above the slices. All the plots are obtained based on the total aggregation of data of all years.

Note that our method interpolates the average rates so that we have estimation for points around which no firms actually exist.

of k flow (the change in number of trading partners), turning the direction of average flows rightward in Fig. 6.

Consistent with the multi-variate scaling, higher sales growth is expected for firms with more employees, ℓ , when the initial sales s and number of trading partners k are controlled (Fig. 6). On the other hand, the effect of increasing the initial number of trading partners, k , on the sales growth is not so visible in the figure. This might be expected from our result above, because $\alpha < \beta$ implies that the gap between the actual sales and the scaled or ‘balanced’ one is larger for firms with more employees rather than for those with more trading partners.

We also notice that those points on the scaling line (Fig. 3a; orange line in Fig. 6) are marked with relatively very slow absolute changes in the activity rate and body sizes: average flows around the point of scaling line are close to zero in comparison to other regions of the variable space (see Supplementary Text 6 for general cases). Therefore, we expect that the growth of firms on the scaling line should be predominantly determined by growth fluctuations and cannot be attributed to their body or activity sizes.

Although we find no direct relation of exit rate to the surface of multi-variate scaling, the scaling line seems to be relevant also to the exit rate of firms, namely, the rate of bankruptcy, merger and suspension or closure of business. For firms of medium or large size, the exit rate exhibits a clear decline around the scaling point (Fig. 7; also see Supplementary Fig. S10). Exit rates are often relatively high for firms that are distant from the scaling line, and at some regions the rates are significantly high, exceeding 3 per cent per year. On the other hand, they are quite low (less than 1 per cent per year) for firms around the scaling line. Thus, deviation from the scaling relations is probably a good sign of higher risk of death.

III. DISCUSSION

We have analyzed the scaling relations inherent in firms and their implications on firm dynamics, highlighting firms’ general tendency towards scaled states in the 3-dimensional space. We first show that firms are densely located in a 2-dimensional scaling surface, and then demonstrate that there exist evolutionary tendencies that leads firms to the surface. We find that the scaling surface is characterized by a clear asymmetry between the slopes of s (sales) versus k (trading partners) or versus ℓ (employees), where the latter is higher. In other words, the number of employees ℓ is more influential to the annual sales s compared to the number of trading partners k . If these quantities are not on the scaling surface, they are, on average, adjusted towards their more ‘balanced’ proportions that abide by the scaling relations. Imbalanced firms also have higher tendency to disappear. This means that the scaling relations are maintained dynamically and would be recovered if they were perturbed. It also follows that only the firms deviat-

ing from the scaling relations have more chance of higher sales growth, but they also suffer from higher risk for disappearance. This matches the intuitive trade-off between risk and return, whereby one cannot avoid taking higher risk when aspiring to attain higher growth (e.g. by increasing recruitment). Of course, this has only partly to do with the whole reality of firms, as random fluctuations in dynamics are prevalent and their increasing employee number does not guarantee positive sales growth, but only increase its chance as evidenced in Fig. 5. The results could be directly applied to the prediction of future firm size, which might benefit investors. Another exciting arena of application might be the control of firm development, such as determination of the growth path that maximizes a firm’s sales growth for a given risk of disappearance that is maximally bearable for entrepreneurs and other stakeholders.

Note that the overall average flow of firms to a more balanced state on the scaling relation surface does not mean that the firm size distribution eventually reduces to a two-dimensional surface or even a one-dimensional curve. There are always temporal fluctuations in firms’ activity rates or sizes. They are the dominant factor of their dynamics especially around the scaling surface (e.g. Fig. 5), and furthermore, distributions of these ‘noises’ are probably fat-tailed, as the plot of size growth rates suggest (see Supplementary Fig. S3). We speculate that diffusion effects of the stochastic growth rates is in equilibrium with the average flows we just find, leading to the unchanging fat-tailed distribution of firms around the scaling relations (Figs. 2b–f) through a process similar to a random multiplicative process[45]. However, the connection between the common scaling function and the stochastic dynamics is yet to be established.

Although we aggregate the data of different years in the evolutionary flow diagrams for the sake of large sample sizes, we find only some small variations when data of different years are compared. One of our important finding is the values of scaling exponents α and β and their variations which seemingly follow the country’s GDP (Fig. 4). The employee number becomes more influential in determining sales in a recovered economy, and the number of trading partners is affecting more (though less than the employee number) in an economic recession compared to other periods. In fact, it is qualitatively convincing that selling whatever produced with labor force would be relatively easy in a recovering economy, while the trading partners to which they could sell their products are more crucial in depression.

We expect that similar results would emerge when applying our method on different datasets of firms from other areas or countries. Tests of this hypothesis would be highly valuable for our understanding of diversity and universality of the firms system. While two-dimensional analysis could be performed without much effort because of the abundant information on the sales and employees, it would be more difficult to conduct a 3-dimensional study of firms in areas other than Japan, since the trad-

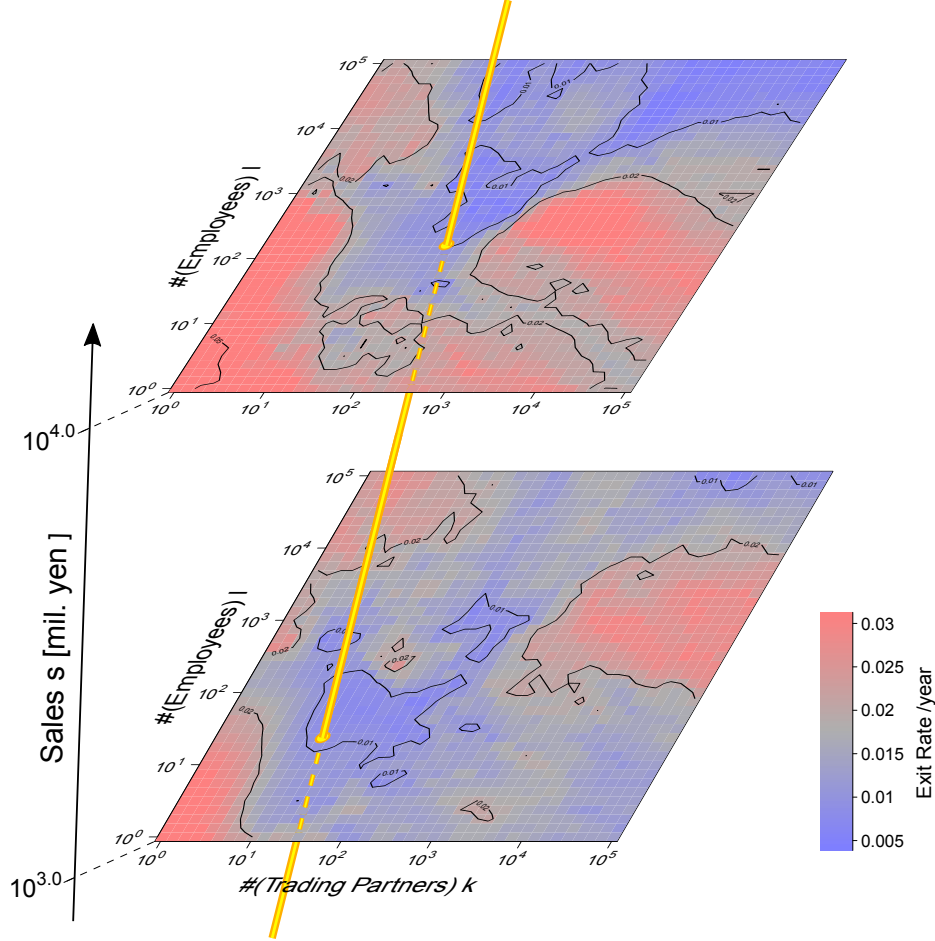


FIG. 7: Illustration of the estimated exit rate per year in slices of the vector space. The variable space is sliced by planes of annual sales s equal to $10^{3.0}$ and $10^{4.0}$ million yen. The estimated exit rate is indicated by the background color, red, grey or blue representing high, medium or low rate of exit, respectively. The orange and yellow line that crosses the slices represents the scaling line of bivariate relations. We add contours to show clearly the regions where exit rates are high or low. The plot is obtained based on the total aggregation of data of all years. Note that our method interpolates the average rates so that we have estimation for points around which no firms actually exists.

ing data are often missing.

Our generalized picture of firm dynamics could serve as a possible guide to a unified understanding of many existing results. For example, it was shown that sales growth become higher for firms just after merging, compared to non-merged firms, and the effect slows down with years[46]. This could be explained as follows. Assume a situation that the employee number and annual sales of a newly merged firm is the sum of those of the antecedents, and that the antecedents were perfectly on the scaling. Then the annual sales should grow on average, since the annual sales is under the level of scaling, given nonlinear increase of sales against employee increment ($\text{sales} \propto \text{employee}^{1.2}$ found empirically). Similarly, higher average growth of entering firms[47, 48] might be explained with their initial out-scaling relation between

their sales and size in employees or trading partners. Thus, generally, the relevance of scaling relations to dynamics found here could explain many features of firm growth. Moreover, the upregulation of company sales after merging is reminiscent of the fact that the metabolic rate per unit mass of a mammalian cell is considerably upregulated when it is cultured *in vitro* with the size of cell clusters far smaller than a mammalian individual[49]. Therefore, the general scaling framework developed here could be useful also for understanding other natural or technological complex organizations.

Presenting novel stylized facts, we believe that our results are also beneficial for future modeling and theory construction. Researchers have formulated numerous models[8, 11, 13–22] to explain a few stylized facts on firms and new criteria were apparently needed to dis-

criminate and validate the models. Thus, we suggest that future theoretical studies should incorporate the phenomenological multi-variate evolution of firm entities found here. Theories for scaling relations between sizes in other complex systems such as animal bodies and cities might be relevant to this enterprise, because fractal-like hierarchical organization is a pervasive design in all these systems[36, 37, 50, 51]. This might open a prospect of devising general understandings and modeling principles for such complex systems.

IV. METHODS

A. Estimating Scaling Exponents

We perform the standard regression analysis with R (ver. 3.1.2)[52] in order to estimate the scaling exponents in the bivariate and multi-variate scaling relationships from the firm data. Bivariate scaling is simply formulated as $x \propto y^\gamma$ (defined in a way similar to Eq. (2); see Supplementary Text 2), where γ is the exponent, and x and y are a pair from those three quantities: the number of trading partners, k , the number of employees, ℓ , and annual sales in million yen, s . On the other hand, multi-variate one is $s \propto k^\alpha \ell^\beta$ (Eq. (2) for definition), where α and β are the scaling exponents of k and ℓ . Although k and ℓ are not mutually independent, regression of s against an orthogonalized set of variables, such as k and $\ell/k^{1.0}$, yields $s \propto k^{\alpha'} (\ell/k^{1.0})^{\beta'}$, which is equivalent to $s \propto k^\alpha \ell^\beta$, where $\alpha = \alpha'^{-1.0} \beta'$ and $\beta = \beta'$ (see Supplementary Text 4 for more discussion). All probability distribution functions of size variables (k , ℓ and s) are fat-tailed for large values in any year (Supplementary Text 1, Supplementary Fig. S2; also see Supplementary Table S1). To avoid extreme values usually seen in variables distributed in such a way, we log-transform the raw size figures, so that the variables are exponentially distributed. After the transformation, the model is linear as defined in Eq. (2). Although the error terms are distributed in a non-Gaussian manner, they are generally invariable regardless of the value of ‘explanatory’ variables (Fig. 2a and Supplementary Figs. S4d–f), and the effect is seemingly linear in larger firms (Figs. 2a–c and 4), so the assumptions of the model Eq. (2) are met. We estimate the exponents for every year of 1994–2015. We exclude the data of firms that lack any of the three variables.

To reject the data of small firms that do not fit to the ‘linear’ assumption of the model (Eq. (2); also see Eqs. (S2.4–6) in Supplementary Text 2), we exclude the data with small k or ℓ by the threshold of 100. This threshold is determined with regard to consistency of the resulting multi-variate scaling exponents to bivariate ones (Supplementary Texts 3 and 4). Although a considerable fraction of data is missed from the analysis (see Supplementary Fig. S5d for final sample sizes), this makes sure that the resulting set of exponents conforms to the model assumptions.

We determine the confidence intervals for the estimates of α and β with the bootstrap technique[53]. Resampling is performed 10,000 times, with the size of resampling being identical to the sample size. Then 95% confidence intervals (CI) are estimated with the 2.5- and 97.5-percentiles of the bootstrap distribution.

B. Differentiation of Growth Correlations

We aim to discriminate between the effects of employee growth and growth in trading partnership on the sales growth. To this end, we compare the firms with a large growth in trading partnership (Group 1) and in employee number (Group 2). ‘Large growth’ is here defined by a growth rate higher than 50%, and the growth of the other variable is controlled within $\pm 20\%$ to expel the effect of correlation between employee and trading partnership growth from the analysis. Sales growth in year t is defined by the ratio of sales s in year t to that in the initial year $t-1$: i.e. $s(t)/s(t-1)$. We consider the ‘accompanying’ sales growth in year t , as well as the ‘following’ sales growth, in year $t+1$. Then, we apply the two-sample Kolmogorov-Smirnov test to the two empirical distributions of sales growth rates from both groups with R (ver. 3.1.2)[52]. Two-tailed test is performed with the significance level of 0.05. Nonparametric tests are favored here, since the distribution is possibly non-Gaussian (Fig. 5) and there is not unanimous agreement on which family of distributions should be fitted against the empirical growth rates[54].

To rule out the possibility that size heterogeneity affects the results, the size variables in the initial year $t-1$ are also controlled. Let us define d_{\log} as a firm’s Euclidean distance in the logarithmically scaled space from a fixed point (k_0, ℓ_0, s_0) in the initial year:

$$d_{\log} = \sqrt{(\log[k(t-1)/k_0])^2 + (\log[\ell(t-1)/\ell_0])^2 + (\log[s(t-1)/s_0])^2}. \quad (5)$$

We include only the firms within the Euclid radius of $d_{\log} < \log[10^{1/8}]$. The fixed point of initial sizes is set on the ‘scaling line’ (Fig. 3a; for the definition, see Eq.

(S6.1) in Supplementary Text 6), to approximately maximize the sample density around the point and to avoid possible biases. A satisfactory sample size is assured by

aggregating the whole data of all years, for which we estimate the scaling exponents α and β as in the above section. Data around the scaling point of $k = 10$ is used to produce the illustrative results in the main text; we address the dependence of results on the k value choice in Supplementary Text 5 (also see Supplementary Fig. S7).

Additionally, we calculate the mean value of log-transformed accompanying or following sales growth rates in these groups. We determine the confidence intervals of the mean again with the bootstrap technique. Here, we apply the same procedures as described in the above section to have 95% CI. We loosely use the term ‘significance’ of difference when no overlap exists between two 95% CI.

C. Estimating Growth and Exit Rates

Here we estimate the medium growth rates of size variables, k , ℓ and s , at a specific point (k_0, ℓ_0, s_0) in the 3-dimensional vector space in order to draw the evolutionary phase diagrams (Fig. 6). We do this again by collecting the data sufficiently near the point and computing the arithmetic mean of log-transformed growth rates. We sample the firms of $d_{\log} < \log[10^{1/4}]$, eventually getting Nadaraya-Watson estimate with the kernel function of rectangular pulse[55]. Nevertheless, when the resulting sample size is less than 200, the threshold of d_{\log} is enlarged until the sample number exceeds 200 to suppress the variability of estimates, therefore employing the 200-nearest neighbor method. Taking the logarithm of growth rates, we can limit their possible ranges of several order of magnitude (Supplementary Text 1, Supplementary Fig. S3) within those expected from exponential distributions, which makes the arithmetic mean a more robust estimator of the typical value. Note that the arithmetic mean of log-transformed growth rates is equal to the logarithm of geometric mean of growth rates.

We use almost the same method for exit rate estimations (Fig. 7), except that the threshold of the sample size is 1,000 rather than 200. This choice is due to the generally low rate of firm exit, only up to 0.03 per year and sometimes lower than 0.01 per year.

Note that the growth rates could be estimated for points around which almost no firms actually exist. In such a case, these estimates are based on the firms on the nearest edge of distribution. Also, be cautious that they are biased when there is gradient of data density: the center of the distribution then has more weight than peripheral regions, so that the effects of moving outward from the center of distribution on growth rate changes are always underestimated.

D. Code Availability

Source codes used in this study is available upon request to the corresponding author, which are written in R language (ver. 3.1.2)[52] and in ShellScript compatible with Red Hat Enterprise Linux Workstation release 7.0 (Red Hat, Raleigh, NC, USA).

E. Data Availability

The data that support the findings of this study are available from Teikoku Databank, Ltd., Japan, but restrictions apply to the availability of these data, which were used under license for the current study, and so are not publicly available. Data are however available from the authors upon reasonable request and with permission of Teikoku Databank, Ltd.

ACKNOWLEDGMENTS

We thank O. Levy for discussions. The authors appreciate Teikoku Databank, Ltd., Center for TDB Advanced Data Analysis and Modeling for providing both the data and financial support. This work is partially supported by the Grant-in-Aid for Scientific Research (B), Grant Number 26310207 and JST, Strategic International Collaborative Research Program (SICORP) on the topic of “ICT for a Resilient Society” by Japan and Israel, and by MEXT as “Exploratory Challenges on Post-K computer (Study on multilayered multiscale spacetime simulations for social and economical phenomena)”.

AUTHOR CONTRIBUTIONS

M.T. directed the project. Y.K., H.T. and S.H. developed the data analysis. Y.K. analyzed the data and generated the diagrams. All authors contributed in writing the paper.

COMPETING INTERESTS

Teikoku Databank, Ltd. supported our research by providing the data regarding Japanese business firms and by financially supporting Center for TDB Advanced Data Analysis and Modeling, Tokyo Institute of Technology for academic research purposes. Teikoku Databank, Ltd. did not participate in our research or preparation of the manuscript except the data collection.

[1] A. Marshall, *Principles of Economics* (Macmillan and Co., New York, 1890).

[2] R. Gibrat, *Les Inégalités Économiques* (Recueil Sirey, Paris, 1931).

- [3] E. T. Penrose, *The Theory of the Growth of the Firm* (Basil Blackwell, Oxford, UK, 1959).
- [4] R. Marris, *The Economic Theory of 'Managerial' Capitalism* (Macmillan, London, 1964).
- [5] A. Coad, *The Growth of Firms: A Survey of Theories and Empirical Evidence* (Edward Elgar, Cheltenham, UK, 2009).
- [6] M. H. R. Stanley, L. A. N. Amaral, S. V. Buldyrev, S. Havlin, H. Leschhorn, P. Maass, M. A. Salinger, and H. E. Stanley, *Nature* **379**, 804 (1996).
- [7] L. A. N. Amaral, S. V. Buldyrev, S. Havlin, P. Maass, M. A. Salinger, H. Eugene Stanley, and M. H. Stanley, *Physica A* **244**, 1 (1997).
- [8] D. Fu, F. Pammolli, S. V. Buldyrev, M. Riccaboni, K. Matia, K. Yamasaki, and H. E. Stanley, *Proceedings of the National Academy of Sciences* **102**, 18801 (2005).
- [9] G. Bottazzi, A. Coad, N. Jacoby, and A. Secchi, *Applied Economics* **43**, 103 (2011).
- [10] G. De Fabritiis, F. Pammolli, and M. Riccaboni, *Physica A* **324**, 38 (2003).
- [11] M. Takayasu, H. Watanabe, and H. Takayasu, *Journal of Statistical Physics* **155**, 47 (2014).
- [12] A. Ishikawa, S. Fujimoto, T. Mizuno, and T. Watanabe, in *Proceedings of the Asia-Pacific Econophysics Conference 2016 — Big Data Analysis and Modeling toward Super Smart Society — (APEC-SSS2016)*, edited by M. Takayasu (Journal of the Physical Society of Japan, Tokyo, 2017) p. 011005.
- [13] S. V. Buldyrev, L. A. Nunes Amaral, S. Havlin, H. Leschhorn, P. Maass, M. A. Salinger, H. Eugene Stanley, and M. H. Stanley, *Journal de Physique I* **7**, 635 (1997), arXiv:9702085 [cond-mat].
- [14] G. Bottazzi and A. Secchi, *Physica A* **324**, 213 (2003).
- [15] S. Alfarano, M. Milaković, A. Irle, and J. Kauschke, *Journal of Economic Dynamics and Control* **36**, 136 (2012).
- [16] M. Gallegati, G. Guilioni, and N. Kichiji, *ICCSA'03 Proceedings of the 2003 international conference on Computational science and its applications* **6**, 770 (2003).
- [17] I. Wright, *Physica A* **346**, 589 (2005), arXiv:0401053 [cond-mat].
- [18] M. Riccaboni, F. Pammolli, S. V. Buldyrev, L. Ponta, and H. E. Stanley, *Proceedings of the National Academy of Sciences* **105**, 19595 (2008), arXiv:0904.1404.
- [19] H. Mondani, P. Holme, and F. Liljeros, *PLoS ONE* **9** (2014), 10.1371/journal.pone.0100527, arXiv:1403.2850.
- [20] O. Malcai, O. Biham, and S. Solomon, *Physical Review E* **60**, 1299 (1999), arXiv:9907320 [cond-mat].
- [21] J. Sutton, *Physica A* **312**, 577 (2002).
- [22] M. Wyart and J. P. Bouchaud, *Physica A* **326**, 241 (2003), arXiv:0210479 [cond-mat].
- [23] A. Coad and R. Rao, *Economics of Innovation and New Technology* **19**, 127 (2010).
- [24] A. Coad and T. Broekel, *Applied Economics* **44**, 1251 (2012).
- [25] Y. U. Saito, T. Watanabe, and M. Iwamura, *Physica A* **383**, 158 (2007).
- [26] H. Watanabe, H. Takayasu, and M. Takayasu, *Physica A* **392**, 741 (2013).
- [27] M. Kleiber, *Physiological Reviews* **27**, 511 (1947).
- [28] W. R. Stahl, *Science* (New York, N.Y.) **150**, 1039 (1965).
- [29] K. Schmidt-Nielsen, *Scaling: Why is Animal Size So Important?* (Cambridge University Press, Cambridge, 1984).
- [30] A. P. Martin and S. R. Palumbi, *Proceedings of the National Academy of Sciences* **90**, 4087 (1993).
- [31] V. M. Savage, J. F. Gillooly, W. H. Woodruff, G. B. West, A. P. Allen, B. J. Enquist, and J. H. Brown, *Functional Ecology* **18**, 257 (2004).
- [32] O. Arrhenius, *The Journal of Ecology* **9**, 95 (1921).
- [33] M. L. Rosenzweig, *Species Diversity in Space and Time* (Cambridge University Press, Cambridge, 1995).
- [34] L. M. A. Bettencourt, J. Lobo, D. Helbing, C. Kuhnert, and G. B. West, *Proceedings of the National Academy of Sciences* **104**, 7301 (2007).
- [35] H. Samaniego and M. E. Moses, *Journal of Transport and Land Use* **1**, 21 (2008).
- [36] X. Li, X. Wang, J. Zhang, and L. Wu, *Palgrave Communications* **1**, 15017 (2015).
- [37] G. B. West, J. H. Brown, and B. J. Enquist, *Science* (New York, N.Y.) **276**, 122 (1997).
- [38] S. D. Yi, J. D. Noh, P. Minnhagen, M. Y. Song, T. S. Chon, and B. J. Kim, *Scientific Reports* **7**, 1 (2017).
- [39] P. Cirillo and J. Hüsler, *Physica A* **388**, 1546 (2009).
- [40] T. Ogwang, *Empirical Economics* **41**, 473 (2011).
- [41] C. P. Klingenberg, *Development Genes and Evolution* **226**, 113 (2016).
- [42] M. Cristelli, A. Tacchella, and L. Pietronero, *PLOS ONE* **10**, e0117174 (2015).
- [43] E. N. Lorenz, *Journal of the Atmospheric Sciences* **26**, 636 (1969).
- [44] E. N. Lorenz, *Bulletin of the American Meteorological Society* **50**, 345 (1969).
- [45] H. Takayasu, A.-H. Sato, and M. Takayasu, *Physical Review Letters* **79**, 966 (1997).
- [46] A. Lockett, J. Wiklund, P. Davidsson, and S. Girma, *Journal of Management Studies* **48**, 48 (2011).
- [47] K. Geurts and J. Van Biesebroeck, *International Journal of Industrial Organization* **49**, 59 (2016).
- [48] B. Gao, W. K. V. Chan, L. Chi, and X. N. Deng, *Electronic Commerce Research and Applications* **17**, 161 (2016).
- [49] G. B. West, W. H. Woodruff, and J. H. Brown, *Proceedings of the National Academy of Sciences* **99**, 2473 (2002).
- [50] M. Batty and P. Longley, *Fractal Cities: A Geometry of Form and Function* (Academic Press, London, 1994).
- [51] B. Fix, *PLoS ONE* **12**, e0171823 (2017).
- [52] R Core Team, "R: A Language and Environment for Statistical Computing," (2014).
- [53] A. Davison and D. Hinkley, *Bootstrap Methods and their Application* (Cambridge University Press, Cambridge, 1997).
- [54] M. A. Williams, B. P. Pinto, and D. Park, *Physica A* **432**, 102 (2015).
- [55] T. Hastie, R. Tibshirani, and J. Friedman, in *The Elements of Statistical Learning: Data Mining, Inference, and Prediction* (Springer, New York, 2009) 2nd ed., Chap. 6, pp. 191–218.

SUPPLEMENTARY MATERIALS

Supplementary Text 1: Data Description

The data employed in this study is the electronic version of COSMOS 2 database, updated yearly each January by Teikoku Databank, Ltd. This database describes over two million business firms in Japan, including two sub-databases: (1) around one million per year ‘summary’ firm profiles such as sales, number of employees and business type category from 1980, and (2) lists of several million trading relationships for each year since 1993. The profile of trading relationships include the direction, that is, which firm (buyer) paid to which (supplier). Only after 1993 the data fully comprehend the multi-dimensional aspect of size and growth of firms and we exclude the 1993 data in order to avoid boundary effects that might be present in 1993 trading data. The data was last updated in January, 2017. This confines our analysis to the period ending in 2015, because the 2016 sales have not been available for all the firms at the time of our study. Every firm has a unique anonymous ID. This enables tracking the firm evolution in time or in different sub-databases. A new ID can be assigned to an existing business activity by corporate reorganization such as an acquisition, a merger, and an identity change.

In order to maintain homogeneity of the included firms at the least level and time coherence between different kinds of data, we perform several steps of data compilation as follows. First, we exclude the firms that are categorized as governmental (e.g. local governments) or financial (e.g. banks and insurers) ones. This is because the definition of sales for these ‘firms’ is quite different from that for construction, manufacturing or wholesale firms, which are the majority of the firms in the data. By this step, we filter out possible outliers in the whole database. This procedure is applied to both sub-databases. Second, we do not use the sales data that are from a financial statement published more than 8 years before the data entry, or those without adequate timestamp. Third, we set the sales to be unknown when the end of fiscal year has changed, because some of such data is supposedly not the annual sales as the value is sometimes considerably less in the fiscal term than in previous or subsequent periods. Fourth, we determine the year to which a sale datum is assigned, according to the year in which the fiscal term ended. For example, when a firm has a fiscal year that started in April, 2000 and ended in March, 2001 like the majority of Japanese firms, sales value of the fiscal term is considered to belong to the year 2001, regardless of whether the data appeared in the database in 2002 or after. In contrast, this is not applied to employees or trading data: we always assign them to the previous year of the data entry, since the database is updated in January every year.

We directly use the raw data without normalization or adjustment for inflation. The number of trading partners of a firm is determined by counting the number of trading relations that a firm participates in the year, regardless of whether the firm is a supplier or a buyer. This amounts to computing the sum of in-degree and out-degree of every node in the directed network of trading.

Firm existence data are additionally compiled to estimate the firm exit rates. First, if any data of a firm exist for a year, the firm is considered to exist in the year. Then, when the data of a firm are not available only

for up to two consecutive years, the firm is also considered to exist in the years where the data are lacking, assuming their absence from the data is a mere consequence of accidents. Before the compilation of the existence data, the first and fourth steps of data exclusion done above for the compilation of quantitative data are also applied to assure the consistency between both datasets.

The data amount before and after the compilation is plotted in Fig. S1 against year during the 1994–2015 period. We note that the data amount is generally increasing. One can see that the number of the firms with complete data of all size variables (i.e. k , l and s) is currently over 0.8 million per year after filtering. The number of existent firms is usually more than that in the sub-database of sales and employees, as the existence is assumed for some firms that only appear in the trading data or ones with temporarily missing data. Two jumps of trading data increase (2007–2008 and 2010–2011) are evident in Fig. S1b. The second jump is due to the data of trading involving financial or governmental organizations, since we see no jump in the same period after the filtering. On the other hand, the first one is the consequence of revised methods of data collection that are only related to trading relations data; trading relations which are mentioned only in on-demand reports became included in the database in 2008. Indeed, there is no comparable jump in the number of ‘summary’ profile data. We also note that the number of exiting or disappearing firms is quite stable compared to the number of entering firms, which implies that the former is less affected by the fluctuation of efforts paid on data collection.

All size variables are distributed in fat-tailed manners at the upper side, as shown in Fig. S2. Their distribution functions for every year are plotted in the figure, with the color gradient from blue through black to red indicating the direction from older data to newer ones. We note that the distributions are fairly stable despite the increase of data and, in particular, the exponents of the power-law tails are evidently invariant. They are respectively -2.2 for k (the number of trading partners), -2.2 for l (employee number) and -2.0 for s (annual sales in million yen). The exponent of sales distribution is consistent with previous studies [1–3]. Consequently, arithmetic mean and standard deviation do not indicate the representative value and the width of the distribution (Table S1). We alternatively measure them by the median and the IQR (interquartile range) in the table. Note, however, that these values are only representative of middle-range values, but not the tails, where considerably regular characteristics appear.

In Fig. S3, we also plot the distribution of firm growth rates $g_x(t) = x(t)/x(t-1)$ of a single variable x in one year, where x is one of the size variables k , l and s and t is the year. The zigzagged forms at the center of k and l distributions in Figs. S3a and S3b are due to the fact that the number of trading partners or employees are integer, and a very large fraction of firms have only a few trading partners or employees (Fig. S2a,b). Again, consistent to the previous studies [4,5], the distributions of log-transformed growth rates $\log[g_x(t)]$ are approximately Laplace or double exponential. This means that the tails of both sides of non-transformed growth rates are approximated with power-laws and one can obtain an extreme value larger or smaller than a unity by several orders of magnitude.

Supplementary Text 2: Scaling between Variables and Universal Distributions

To assure that the scaling relationships that were found in the previous study [6] are also present in our data, we follow the methodology described there to replicate their results. The data in the previous study were independently gathered from the data provider in our study, Teikoku Databank, Ltd. However, we expect that similar results would emerge, as data are collected for the same system (i.e. the Japanese firms) in both datasets.

Firstly, we confirm the following scaling relationships, which is defined in terms of conditional distributions [6]:

$$P(l|k) = \tilde{P}_{l|k}(l/k^{\gamma_1})/k^{\gamma_1}, \quad (\text{S2.1})$$

$$P(s|k) = \tilde{P}_{s|k}(s/k^{\gamma_2})/k^{\gamma_2}, \quad (\text{S2.2})$$

$$P(s|l) = \tilde{P}_{s|l}(s/l^{\gamma_3})/l^{\gamma_3}, \quad (\text{S2.3})$$

where $P(x|y)$ is the probability density function of the variable x conditional on a specific y -value, γ_1 , γ_2 and γ_3 are the scaling exponents, and $\tilde{P}_{x|y}$ is a scaling function for variable x conditional on the y -value, which represents the distribution of fluctuation ratio around the scaling line, $x \propto y^\gamma$. These relations are equivalent to the more intuitive regression-type formulae as shown in Supplementary Text 4:

$$\log l = \gamma_1 \log k + \varepsilon_{l|k}, \quad (\text{S2.4})$$

$$\log s = \gamma_2 \log k + \varepsilon_{s|k}, \quad (\text{S2.5})$$

$$\log s = \gamma_3 \log l + \varepsilon_{s|l}, \quad (\text{S2.6})$$

where the error terms, $\varepsilon_{l|k}$, $\varepsilon_{s|k}$ and $\varepsilon_{s|l}$, can be regarded as stochastic variables (including the intercept term) that correspond to $\tilde{P}_{l|k}$, $\tilde{P}_{s|k}$ and $\tilde{P}_{s|l}$. These formulae are naturally interpreted as projections of a single 3-dimensional scaling line, where the firms are densely distributed, to the 2-dimensional planes (Fig. 3a).

To test the validity of these relationships (Eqs. (S2.1–6)) in our data, we examine both the conditional quantiles (Fig. S4a–c) and the distributions of the error terms (Fig. S4d–f), where the conditional quantile is defined as follows: for any given number q in the range of (0, 1), the q -quantile of x conditional on y , denoted as $\langle x|y \rangle_q$, is defined by the value that fulfills the following equation,

$$\int_0^{\langle x|y \rangle_q} P(x|y) dx = q. \quad (\text{S2.7})$$

As shown in Fig. S4a–c, the plots of $\log \langle x|y \rangle_q$ vs $\log y$ show linear relations for a wide range of y , meaning that the power law relation, $\langle x|y \rangle_q \propto y^\gamma$, shortly denoted by $x \propto y^\gamma$, holds for all combinations of k , l and s . We estimate the values of exponents as $\gamma_1 \sim 1.0$, $\gamma_2 \sim 1.2$, and $\gamma_3 \sim 1.2$ (Supplementary Text 4). In Fig. S4d–f, we plot the scaling functions, $\tilde{P}_{x|y}$, for 8 intervals of a logarithmically equal range of y , and confirm that all the curves collapse into a single scaling function for all three cases, demonstrating the validity of the scaling relations of Eqs. (S2.1–3).

Supplementary Text 3: Derivation of Asymptotic Power-law or Scaling Exponents

In this note, we derive the asymptotic exponents of power-law distributions and scaling relationships from other

ones to check the consistency of our results. First, given Eqs. (S2.1–3), we derive the asymptotic power-law exponent of the marginal distribution $P(x)$ of the ‘explained’ variable x . Second, assuming Eqs. (3) and (S2.1), we calculate the asymptotic power-law exponent of marginal distribution of s . Third, we show that the bivariate scaling exponents γ_2 and γ_3 (i.e. those of the sales s against the number of trading partners k and against employee number l respectively) can be determined from α , β and γ_1 .

Since Eqs. (S2.1–3) have the general form

$$P(x|y) = \tilde{P}_{x|y}(x/y^\gamma)/y^\gamma, \quad (\text{S3.1})$$

we can derive the power-law exponent of the marginal distribution $P_x(x)$ of a variable x from the following three: the positive scaling exponent γ , $\tilde{P}_{x|y}$ (the universal distribution function of x conditional on y) and the marginal distribution $P_y(y)$. Assuming that $\tilde{P}_{x|y}$ and P_y has a power-law upper tail of exponent $\delta_{x|y}$ and δ_y , we approximate the functions as

$$\tilde{P}_{x|y}(\tilde{x}) = \begin{cases} c_{x|y}\tilde{x}^{-\delta_{x|y}} & (\tilde{x} \geq 1) \\ d_{x|y}(\tilde{x}) & (0 \leq \tilde{x} < 1) \end{cases} \quad (\text{S3.2})$$

and

$$P_y(y) = \begin{cases} c_y y^{-\delta_y} & (y \geq 1) \\ d_y(y) & (0 \leq y < 1) \end{cases}, \quad (\text{S3.3})$$

where $c_{x|y}$ and c_y are positive constants, $\delta_{x|y}$ and δ_y are the power-law exponents larger than 1 and $d_{x|y}$ and d_y are the distribution functions at the smaller side. This approximation is motivated by the actual distributions of size variables (Figs. 2d–f and S2). We set the threshold beyond which the distribution follow the power law to 1, since, otherwise, the same results are easily derived for the asymptotic value of exponents with linear transformations.

Applying Bayes’ theorem and assuming $x > 1$ (as we are interested in the ‘tails’ or asymptotic behaviors at $x \rightarrow \infty$), we derive $P_x(x)$, the marginal distribution of x , from $P(x, y)$, the joint distribution of x and y :

$$\begin{aligned} P_x(x) &= \int_0^\infty P(x, y) dy = \int_0^\infty P(x|y) P(y) dy = \int_0^\infty \frac{1}{y^\gamma} \tilde{P}_{x|y}\left(\frac{x}{y^\gamma}\right) P_y(y) dy \\ &= \int_0^1 \frac{1}{y^\gamma} c_{x|y} \left(\frac{x}{y^\gamma}\right)^{-\delta_{x|y}} d_y(y) dy + \int_1^{x^{1/\gamma}} \frac{1}{y^\gamma} c_{x|y} \left(\frac{x}{y^\gamma}\right)^{-\delta_{x|y}} c_y y^{-\delta_y} dy + \int_{x^{1/\gamma}}^\infty \frac{1}{y^\gamma} d_{x|y}\left(\frac{x}{y^\gamma}\right) c_y y^{-\delta_y} dy \\ &= c_{x|y} x^{-\delta_{x|y}} \int_0^1 y^{\gamma(\delta_{x|y}-1)} d_y(y) dy + c_{x|y} c_y x^{-\delta_{x|y}} \int_1^{x^{1/\gamma}} y^{\gamma(\delta_{x|y}-1)-\delta_y} dy \\ &\quad + c_y x^{-(\delta_y-1)/\gamma-1} \int_1^\infty \tilde{y}^{-\gamma-\delta_y} d_{x|y}\left(\frac{1}{\tilde{y}^\gamma}\right) d\tilde{y} \\ &= (I_1 - C) x^{-\delta_{x|y}} + (I_2 + C) x^{-1-(\delta_y-1)/\gamma}, \end{aligned}$$

where I_1 , I_2 and C are constants defined as

$$I_1 = c_{x|y} \int_0^1 y^{\gamma(\delta_{x|y}-1)} d_y(y) dy,$$

$$I_2 = c_y \int_1^\infty \tilde{y}^{-\gamma-\delta_y} d_{x|y} \left(\frac{1}{\tilde{y}^\gamma} \right) d\tilde{y},$$

$$C = c_{x|y} c_y / (\gamma(\delta_{x|y} - 1) - \delta_y + 1),$$

and the substitution $\tilde{y} = y/x^{1/\gamma}$ is applied in the last integral term. Therefore, the asymptotic behavior of $P_x(x)$ at positive infinity is determined by which of $-\delta_{x|y}$ and $-1 - (\delta_y - 1)/\gamma$ is the larger: when $x \rightarrow \infty$, the behavior of P_x is approximated with

$$P_x(x) \propto x^{-\delta_x}, \quad (\text{S3.4})$$

where

$$-\delta_x = \max \left[-\delta_{x|y}, -1 - \frac{\delta_y - 1}{\gamma} \right]. \quad (\text{S3.5})$$

Note that change of $\delta_{x|y}$ does not have any effect on the power-law exponent as far as δ_y is sufficiently large, which is consistent to the intuitive explanation (Fig. 1) in the main text.

Although somewhat complicated, a similar strategy works for the case of multi-variate scaling. Let us continue with the above notations except that x, y and γ are respectively replaced with l, k and γ_1 , and assume Eq. (3) as well as the following:

$$\tilde{P}_{s|k,l}(\tilde{s}) = \begin{cases} c_{s|k,l} \tilde{s}^{-\delta_{s|k,l}} & (\tilde{s} \geq 1) \\ d_{s|k,l}(\tilde{s}) & (0 \leq \tilde{s} < 1) \end{cases}, \quad (\text{S3.6})$$

where $c_{s|k,l}$ is a positive constant, $\delta_{s|k,l}$ the power-law exponent larger than 1 and $d_{s|k,l}$ the distribution function at the smaller side. Again, the threshold of the functional change of $\tilde{P}_{s|k,l}$ is set to a unity without loss of generality. The marginal distribution of s , $P_s(s)$, for $s > 1$ is

$$P_s(s) = \int_0^\infty \int_0^\infty P(k, l, s) dl dk = \int_0^\infty \int_0^\infty P(s|k, l) P(k, l) dl dk = \int_0^\infty \int_0^\infty P(s|k, l) P(l|k) P(k) dl dk.$$

Then, this is calculated as the sum of following ten integral terms:

$$\begin{aligned} \int_0^1 \int_0^{k^{\gamma_1}} P(s|k, l) P(l|k) P(k) dl dk &= \int_0^1 \int_0^{k^{\gamma_1}} \frac{1}{k^{\alpha} l^{\beta}} c_{s|k,l} \left(\frac{s}{k^{\alpha} l^{\beta}} \right)^{-\delta_{s|k,l}} \frac{1}{k^{\gamma_1}} d_{l|k} \left(\frac{l}{k^{\gamma_1}} \right) d_k(k) dl dk \\ &= c_{s|k,l} s^{-\delta_{s|k,l}} \int_0^1 k^{-\gamma_1 + \alpha(\delta_{s|k,l} - 1)} d_k(k) \int_0^{k^{\gamma_1}} l^{\beta(\delta_{s|k,l} - 1)} d_{l|k} \left(\frac{l}{k^{\gamma_1}} \right) dl dk \\ &= \left[c_{s|k,l} \int_0^1 k^{(\alpha + \beta\gamma_1)(\delta_{s|k,l} - 1)} d_k(k) \int_0^1 \tilde{l}^{\beta(\delta_{s|k,l} - 1)} d_{l|k}(\tilde{l}) d\tilde{l} dk \right] s^{-\delta_{s|k,l}}, \end{aligned}$$

where the substitution $\tilde{l} = l/k^{\gamma_1}$ is applied;

$$\begin{aligned} &\int_0^1 \int_{k^{\gamma_1}}^{(s/k^{\alpha})^{1/\beta}} P(s|k, l) P(l|k) P(k) dl dk \\ &= \int_0^1 \int_{k^{\gamma_1}}^{(s/k^{\alpha})^{1/\beta}} \frac{1}{k^{\alpha} l^{\beta}} c_{s|k,l} \left(\frac{s}{k^{\alpha} l^{\beta}} \right)^{-\delta_{s|k,l}} \frac{1}{k^{\gamma_1}} c_{l|k} \left(\frac{l}{k^{\gamma_1}} \right)^{-\delta_{l|k}} d_k(k) dl dk \\ &= c_{l|k} c_{s|k,l} s^{-\delta_{s|k,l}} \int_0^1 k^{\alpha(\delta_{s|k,l} - 1) + \gamma_1(\delta_{l|k} - 1)} d_k(k) \int_{k^{\gamma_1}}^{(s/k^{\alpha})^{1/\beta}} l^{\beta(\delta_{s|k,l} - 1) - \delta_{l|k}} dl dk \end{aligned}$$

$$= \frac{c_{l|k} c_{s|k,l}}{E_1} \left(\left[\int_0^1 k^{(\alpha/\beta + \gamma_1)(\delta_{l|k}-1)} d_k(k) dk \right] s^{-1-(\delta_{l|k}-1)/\beta} - \left[\int_0^1 k^{(\alpha + \beta \gamma_1)(\delta_{s|k,l}-1)} d_k(k) dk \right] s^{-\delta_{s|k,l}} \right),$$

where $E_1 = \beta(\delta_{s|k,l} - 1) - \delta_{l|k} + 1$;

$$\begin{aligned} \int_0^1 \int_{\left(\frac{s}{k}\right)^{\frac{1}{\beta}}}^{\infty} P(s|k,l) P(l|k) P(k) dl dk &= \int_0^1 \int_{\left(\frac{s}{k}\right)^{\frac{1}{\beta}}}^{\infty} \frac{1}{k^{\alpha} l^{\beta}} d_{s|k,l} \left(\frac{s}{k^{\alpha} l^{\beta}} \right) \frac{1}{k^{\gamma_1}} c_{l|k} \left(\frac{l}{k^{\gamma_1}} \right)^{-\delta_{l|k}} d_k(k) dl dk \\ &= c_{l|k} \int_0^1 k^{\gamma_1(\delta_{l|k}-1)-\alpha} d_k(k) \int_{(s/k^{\alpha})^{1/\beta}}^{\infty} d_{s|k,l} \left(\frac{s}{k^{\alpha} l^{\beta}} \right) l^{-\delta_{l|k}-\beta} dl dk \\ &= \left[c_{l|k} \int_0^1 k^{(\alpha/\beta + \gamma_1)(\delta_{l|k}-1)} d_k(k) dk \int_1^{\infty} d_{s|k,l} \left(\frac{1}{\tilde{l}^{\beta}} \right) \tilde{l}^{-\delta_{l|k}-\beta} d\tilde{l} \right] s^{-1-(\delta_{l|k}-1)/\beta}, \end{aligned}$$

where the substitution $\tilde{l} = (k^{\alpha/\beta} / s^{1/\beta}) \cdot l$ is applied;

$$\begin{aligned} \int_1^{s^{1/(\alpha + \beta \gamma_1)}} \int_0^{k^{\gamma_1}} P(s|k,l) P(l|k) P(k) dl dk &= \int_1^{s^{1/(\alpha + \beta \gamma_1)}} \int_0^{k^{\gamma_1}} \frac{1}{k^{\alpha} l^{\beta}} c_{s|k,l} \left(\frac{s}{k^{\alpha} l^{\beta}} \right)^{-\delta_{s|k,l}} \frac{1}{k^{\gamma_1}} d_{l|k} \left(\frac{l}{k^{\gamma_1}} \right) c_k k^{-\delta_k} dl dk \\ &= c_k c_{s|k,l} s^{-\delta_{s|k,l}} \int_1^{s^{1/(\alpha + \beta \gamma_1)}} k^{\alpha(\delta_{s|k,l}-1)-\gamma_1-\delta_k} \int_0^{k^{\gamma_1}} l^{\beta(\delta_{s|k,l}-1)} d_{l|k} \left(\frac{l}{k^{\gamma_1}} \right) dl dk \\ &= \frac{c_k c_{s|k,l}}{E_2} \left[\int_0^1 \tilde{l}^{\beta(\delta_{s|k,l}-1)} d_{l|k}(\tilde{l}) d\tilde{l} \right] (s^{-1-(\delta_k-1)/(\alpha + \beta \gamma_1)} - s^{-\delta_{s|k,l}}), \end{aligned}$$

where the substitution $\tilde{l} = l/k^{\gamma_1}$ is applied and $E_2 = (\alpha + \beta \gamma_1)(\delta_{s|k,l} - 1) - \delta_k + 1$;

$$\begin{aligned} \int_1^{s^{1/(\alpha + \beta \gamma_1)}} \int_{k^{\gamma_1}}^{(s/k^{\alpha})^{1/\beta}} P(s|k,l) P(l|k) P(k) dl dk &= \int_1^{s^{1/(\alpha + \beta \gamma_1)}} \int_{k^{\gamma_1}}^{(s/k^{\alpha})^{1/\beta}} \frac{1}{k^{\alpha} l^{\beta}} c_{s|k,l} \left(\frac{s}{k^{\alpha} l^{\beta}} \right)^{-\delta_{s|k,l}} \frac{1}{k^{\gamma_1}} c_{l|k} \left(\frac{l}{k^{\gamma_1}} \right)^{-\delta_{l|k}} c_k k^{-\delta_k} dl dk \\ &= c_k c_{l|k} c_{s|k,l} s^{-\delta_{s|k,l}} \int_1^{s^{1/(\alpha + \beta \gamma_1)}} k^{\alpha(\delta_{s|k,l}-1) + \gamma_1(\delta_{l|k}-1) - \delta_k} \int_{k^{\gamma_1}}^{(s/k^{\alpha})^{1/\beta}} l^{\beta(\delta_{s|k,l}-1) - \delta_{l|k}} dl dk \\ &= \frac{c_k c_{l|k} c_{s|k,l}}{E_1} \left(\left(\frac{1}{E_3} - \frac{1}{E_2} \right) s^{-1-(\delta_k-1)/(\alpha + \beta \gamma_1)} - \frac{1}{E_3} s^{-1-(\delta_{l|k}-1)/\beta} + \frac{1}{E_2} s^{-\delta_{s|k,l}} \right), \end{aligned}$$

where $E_3 = (\alpha/\beta + \gamma_1)(\delta_{l|k} - 1) - \delta_k + 1$;

$$\begin{aligned} \int_1^{s^{1/(\alpha + \beta \gamma_1)}} \int_{(s/k^{\alpha})^{1/\beta}}^{\infty} P(s|k,l) P(l|k) P(k) dl dk &= \int_1^{s^{1/(\alpha + \beta \gamma_1)}} \int_{(s/k^{\alpha})^{1/\beta}}^{\infty} \frac{1}{k^{\alpha} l^{\beta}} d_{s|k,l} \left(\frac{s}{k^{\alpha} l^{\beta}} \right) \frac{1}{k^{\gamma_1}} c_{l|k} \left(\frac{l}{k^{\gamma_1}} \right)^{-\delta_{l|k}} c_k k^{-\delta_k} dl dk \\ &= c_k c_{l|k} \int_1^{s^{1/(\alpha + \beta \gamma_1)}} k^{-\alpha + \gamma_1(\delta_{l|k}-1) - \delta_k} \int_{(s/k^{\alpha})^{1/\beta}}^{\infty} \frac{1}{\tilde{l}^{\beta}} d_{s|k,l} \left(\frac{s}{k^{\alpha} \tilde{l}^{\beta}} \right) \tilde{l}^{-\delta_{l|k}} d\tilde{l} dk \\ &= \left[\frac{c_k c_{l|k}}{E_3} \int_1^{\infty} d_{s|k,l} \left(\frac{1}{\tilde{l}^{\beta}} \right) \tilde{l}^{-\delta_{l|k}-\beta} d\tilde{l} \right] (s^{-1-(\delta_k-1)/(\alpha + \beta \gamma_1)} - s^{-1-(\delta_{l|k}-1)/\beta}), \end{aligned}$$

where the substitution $\tilde{l} = (k^{\alpha/\beta}/s^{1/\beta}) \cdot l$ is applied;

$$\begin{aligned} & \int_0^{s^{\gamma_1/(\alpha+\beta\gamma_1)}} \int_{s^{1/(\alpha+\beta\gamma_1)}}^{(s/l^\beta)^{1/\alpha}} P(s|k, l)P(l|k)P(k)dk dl \\ &= \int_0^{s^{\gamma_1/(\alpha+\beta\gamma_1)}} \int_{s^{1/(\alpha+\beta\gamma_1)}}^{(s/l^\beta)^{1/\alpha}} \frac{1}{k^\alpha l^\beta} c_{s|k, l} \left(\frac{s}{k^\alpha l^\beta} \right)^{-\delta_{s|k, l}} \frac{1}{k^{\gamma_1}} d_{l|k} \left(\frac{l}{k^{\gamma_1}} \right) c_k k^{-\delta_k} dk dl \\ &= (c_k c_{s|k, l} I_1^3) s^{-1-(\delta_k-1)/(\alpha+\beta\gamma_1)}, \end{aligned}$$

where

$$I_1^3 = \int_0^1 \tilde{l}^{-1+(\delta_{s|k, l}-1)(\alpha+\beta\gamma_1)/\gamma_1-(\delta_k-1)/\gamma_1} \int_{\tilde{l}^{-1/\gamma_1}}^{\tilde{l}^{-(\alpha+\beta\gamma_1)/\alpha\gamma_1}} \tilde{k}^{\alpha(\delta_{s|k, l}-1)-\gamma_1-\delta_k} d_{l|k} \left(\frac{1}{\tilde{k}^{\gamma_1}} \right) d\tilde{k} d\tilde{l}$$

and the substitutions $\tilde{k} = l^{-1/\gamma_1} \cdot k$ and $\tilde{l} = s^{-\gamma_1/(\alpha+\beta\gamma_1)} \cdot l$ are applied;

$$\begin{aligned} & \int_0^{s^{\gamma_1/(\alpha+\beta\gamma_1)}} \int_{(s/l^\beta)^{1/\alpha}}^\infty P(s|k, l)P(l|k)P(k)dk dl \\ &= \int_0^{s^{\gamma_1/(\alpha+\beta\gamma_1)}} \int_{(s/l^\beta)^{1/\alpha}}^\infty \frac{1}{k^\alpha l^\beta} d_{s|k, l} \left(\frac{s}{k^\alpha l^\beta} \right) \frac{1}{k^{\gamma_1}} d_{l|k} \left(\frac{l}{k^{\gamma_1}} \right) c_k k^{-\delta_k} dk dl \\ &= (c_k I_2^3) s^{-1-(\delta_k-1)/(\alpha+\beta\gamma_1)}, \end{aligned}$$

where

$$I_2^3 = \int_0^1 \tilde{l}^{(\gamma_1+\delta_k-1)\beta/\alpha} \int_1^\infty \frac{1}{\tilde{k}^\alpha} d_{s|k, l} \left(\frac{1}{\tilde{k}^\alpha} \right) \frac{1}{\tilde{k}^{\gamma_1}} d_{s|k, l} \left(\frac{\tilde{l}^{(\alpha+\beta\gamma_1)/\alpha}}{\tilde{k}^{\gamma_1}} \right) \tilde{k}^{-\delta_k} d\tilde{k} d\tilde{l}$$

and the substitutions $\tilde{k} = (l^\beta/s)^{1/\alpha} \cdot k$ and $\tilde{l} = s^{-\gamma_1/(\alpha+\beta\gamma_1)} \cdot l$ are applied;

$$\begin{aligned} & \int_{s^{\gamma_1/(\alpha+\beta\gamma_1)}}^\infty \int_{l^{1/\gamma_1}}^\infty P(s|k, l)P(l|k)P(k)dk dl \\ &= \int_{s^{\gamma_1/(\alpha+\beta\gamma_1)}}^\infty \int_{l^{1/\gamma_1}}^\infty \frac{1}{k^\alpha l^\beta} d_{s|k, l} \left(\frac{s}{k^\alpha l^\beta} \right) \frac{1}{k^{\gamma_1}} d_{l|k} \left(\frac{l}{k^{\gamma_1}} \right) c_k k^{-\delta_k} dk dl \\ &= (c_k I_3^3) s^{-1-(\delta_k-1)/(\alpha+\beta\gamma_1)}, \end{aligned}$$

where

$$I_3^3 = \int_1^\infty \tilde{l}^{-1-(\alpha+\beta\gamma_1+\delta_k-1)/\gamma_1} \int_1^\infty \frac{1}{\tilde{k}^\alpha} d_{s|k, l} \left(\frac{1}{\tilde{k}^\alpha \tilde{l}^{(\alpha+\beta\gamma_1)/\gamma_1}} \right) \frac{1}{\tilde{k}^{\gamma_1}} d_{s|k, l} \left(\frac{1}{\tilde{k}^{\gamma_1}} \right) \tilde{k}^{-\delta_k} d\tilde{k} d\tilde{l}$$

and the substitutions $\tilde{k} = l^{-1/\gamma_1} \cdot k$ and $\tilde{l} = s^{-\gamma_1/(\alpha+\beta\gamma_1)} \cdot l$ are applied;

$$\begin{aligned} & \int_{s^{\gamma_1/(\alpha+\beta\gamma_1)}}^\infty \int_{s^{1/(\alpha+\beta\gamma_1)}}^{l^{1/\gamma_1}} P(s|k, l)P(l|k)P(k)dk dl \\ &= \int_{s^{\gamma_1/(\alpha+\beta\gamma_1)}}^\infty \int_{s^{1/(\alpha+\beta\gamma_1)}}^{l^{1/\gamma_1}} \frac{1}{k^\alpha l^\beta} d_{s|k, l} \left(\frac{s}{k^\alpha l^\beta} \right) \frac{1}{k^{\gamma_1}} c_{l|k} \left(\frac{l}{k^{\gamma_1}} \right)^{-\delta_{l|k}} c_k k^{-\delta_k} dk dl \\ &= (c_k c_{l|k} I_4^3) s^{-1-(\delta_k-1)/(\alpha+\beta\gamma_1)}, \end{aligned}$$

where

$$I_4^3 = \int_1^\infty \tilde{l}^{-1-(\alpha+\beta\gamma_1+\delta_k-1)/\gamma_1} \int_{\tilde{l}^{-1/\gamma_1}}^1 \frac{1}{\tilde{k}^\alpha} d_{s|k, l} \left(\frac{1}{\tilde{k}^\alpha \tilde{l}^{(\alpha+\beta\gamma_1)/\gamma_1}} \right) \tilde{k}^{\gamma_1(\delta_{l|k}-1)-\delta_k} d\tilde{k} d\tilde{l}$$

and the substitutions $\tilde{k} = l^{-1/\gamma_1} \cdot k$ and $\tilde{l} = s^{-\gamma_1/(\alpha+\beta\gamma_1)} \cdot l$ are applied. We note that the final sum of these ten terms has the form

$$P_s(s) = A_1 \cdot s^{-\delta_{s|k,l}} + A_2 \cdot s^{-1-\frac{\delta_{l|k}-1}{\beta}} + A_3 \cdot s^{-1-\frac{\delta_k-1}{\alpha+\beta\gamma_1}},$$

where A_1 , A_2 and A_3 are independent of s . Therefore, the asymptotic behavior of P_s at $s \rightarrow \infty$ is that

$$P_s(s) \propto s^{-\delta_s}, \quad (\text{S3.7})$$

where $-\delta_s$ is the largest of the three exponents:

$$-\delta_s = \max \left[-\delta_{s|k,l}, \quad -1 - \frac{\delta_{l|k}-1}{\beta}, \quad -1 - \frac{\delta_k-1}{\alpha+\beta\gamma_1} \right]. \quad (\text{S3.8})$$

Lastly, we evaluate the values of the exponents γ_2 and γ_3 from α , β and γ_1 . Again, assume Eqs. (2) and (S2.1). Then, the joint distribution of k , l and s is given by

$$P(k, l, s) = P(s|k, l)P(l|k)P(k) = \frac{1}{k^\alpha l^\beta} \tilde{P}_{s|k,l} \left(\frac{s}{k^\alpha l^\beta} \right) \frac{1}{k^{\gamma_1}} \tilde{P}_{l|k} \left(\frac{l}{k^{\gamma_1}} \right) P_k(k).$$

We can obtain the joint distribution of k and s by integrating this probability by l .

$$P(k, s) = \int_{-\infty}^{\infty} P(k, l, s) dl = \int_0^{\infty} \frac{1}{k^\alpha l^\beta} \tilde{P}_{s|k,l} \left(\frac{s}{k^\alpha l^\beta} \right) \frac{1}{k^{\gamma_1}} \tilde{P}_{l|k} \left(\frac{l}{k^{\gamma_1}} \right) P_k(k) dl.$$

Now,

$$P(k = k_0, s) = \int_0^{\infty} \frac{1}{k_0^\alpha l^\beta} \tilde{P}_{s|k,l} \left(\frac{s}{k_0^\alpha l^\beta} \right) \frac{1}{k_0^{\gamma_1}} \tilde{P}_{l|k} \left(\frac{l}{k_0^{\gamma_1}} \right) P_k(k_0) dl$$

and

$$\begin{aligned} P(k = k_1, s) &= \int_0^{\infty} \frac{1}{k_1^\alpha l^\beta} \tilde{P}_{s|k,l} \left(\frac{s}{k_1^\alpha l^\beta} \right) \frac{1}{k_1^{\gamma_1}} \tilde{P}_{l|k} \left(\frac{l}{k_1^{\gamma_1}} \right) P_k(k_1) dl \\ &= \left(\frac{k_0}{k_1} \right)^{\alpha+\beta\gamma_1} \cdot \frac{P_k(k_1)}{P_k(k_0)} \int_0^{\infty} \frac{1}{k_0^\alpha \tilde{l}^\beta} \tilde{P}_{s|k,l} \left(\frac{s}{k_0^\alpha \tilde{l}^\beta} \cdot \left(\frac{k_0}{k_1} \right)^{\alpha+\beta\gamma_1} \right) \frac{1}{k_0^{\gamma_1}} \tilde{P}_{l|k} \left(\frac{\tilde{l}}{k_0^{\gamma_1}} \right) P_k(k_0) d\tilde{l} \\ &= \left(\frac{k_0}{k_1} \right)^{\alpha+\beta\gamma_1} \cdot \frac{P_k(k_1)}{P_k(k_0)} \cdot P \left(k = k_0, \quad s = \left(\frac{k_0}{k_1} \right)^{\alpha+\beta\gamma_1} s \right), \end{aligned}$$

where the substitution $\tilde{l} = (k_0/k_1)^{\gamma_1} \cdot l$ is used. Here,

$$\begin{aligned} P(s|k = k_1) &= \frac{P(s, k_1)}{P(k_1)} = \frac{1}{k_1^{\alpha+\beta\gamma_1}} \cdot \frac{k_0^{\alpha+\beta\gamma_1}}{P_k(k_0)} \cdot P \left(k = k_0, \quad s = k_0^{\alpha+\beta\gamma_1} \cdot \frac{s}{k_1^{\alpha+\beta\gamma_1}} \right) \\ &= \frac{1}{k_1^{\alpha+\beta\gamma_1}} \tilde{P}_{s|k} \left(\frac{s}{k_1^{\alpha+\beta\gamma_1}} \right), \end{aligned}$$

where

$$\tilde{P}_{s|k}(\tilde{s}) = \frac{k_0^{\alpha+\beta\gamma_1}}{P_k(k_0)} \cdot P(k = k_0, \quad s = k_0^{\alpha+\beta\gamma_1} \cdot \tilde{s}).$$

Comparing the result above with Eq. (S2.2), we have

$$\gamma_2 = \alpha + \beta\gamma_1. \quad (\text{S3.9})$$

Similarly, the joint distribution of l and s is determined with the equation

$$P(l, s) = \int_{-\infty}^{\infty} P(k, l, s) dk = \int_0^{\infty} \frac{1}{k^{\alpha} l^{\beta}} \tilde{P}_{s|k,l} \left(\frac{s}{k^{\alpha} l^{\beta}} \right) \frac{1}{k^{\gamma_1}} \tilde{P}_{l|k} \left(\frac{l}{k^{\gamma_1}} \right) P_k(k) dk,$$

and, as a result,

$$P(l = l_0, s) = \int_0^{\infty} \frac{1}{k^{\alpha} l_0^{\beta}} \tilde{P}_{s|k,l} \left(\frac{s}{k^{\alpha} l_0^{\beta}} \right) \frac{1}{k^{\gamma_1}} \tilde{P}_{l|k} \left(\frac{l}{k^{\gamma_1}} \right) P_k(k) dk$$

and

$$\begin{aligned} P(l = l_1, s) &= \int_0^{\infty} \frac{1}{k^{\alpha} l_1^{\beta}} \tilde{P}_{s|k,l} \left(\frac{s}{k^{\alpha} l_1^{\beta}} \right) \frac{1}{k^{\gamma_1}} \tilde{P}_{l|k} \left(\frac{l}{k^{\gamma_1}} \right) P_k(k) dk \\ &= \left(\frac{l_0}{l_1} \right)^{(\gamma_1 - 1 + \alpha + \beta \gamma_1)/\gamma_1} \cdot \int_0^{\infty} \frac{1}{\tilde{k}^{\alpha} l_0^{\beta}} \tilde{P}_{s|k,l} \left(\frac{s}{\tilde{k}^{\alpha} l_0^{\beta}} \cdot \left(\frac{l_0}{l_1} \right)^{(\alpha + \beta \gamma_1)/\gamma_1} \right) \frac{1}{\tilde{k}^{\gamma_1}} \tilde{P}_{l|k} \left(\frac{l_0}{\tilde{k}^{\gamma_1}} \right) P_k \left(\tilde{k} \cdot \left(\frac{l_1}{l_0} \right)^{1/\gamma_1} \right) d\tilde{k}, \end{aligned}$$

where the substitution $\tilde{k} = (l_0/l_1)^{1/\gamma_1} \cdot k$ is used. Then, if we assume the power law distribution of k comparable to Eq. (S3.3), namely

$$P_k(k) = \begin{cases} c_k k^{-\delta_k} & (y \geq \theta_k) \\ d_k(k) & (0 \leq y < \theta_k) \end{cases},$$

where θ_k is a positive constant of the threshold,

$$\begin{aligned} P(l = l_1, s) &= \left(\frac{l_0}{l_1} \right)^{(\gamma_1 - 1 + \alpha + \beta \gamma_1)/\gamma_1} \left[\left(\frac{l_0}{l_1} \right)^{\delta_k/\gamma_1} P \left(l = l_0, \left(\frac{l_0}{l_1} \right)^{(\alpha + \beta \gamma_1)/\gamma_1} s \right) \right. \\ &\quad \left. - \int_0^{\theta_k} \frac{1}{\tilde{k}^{\alpha} l_0^{\beta}} \tilde{P}_{s|k,l} \left(\frac{s}{\tilde{k}^{\alpha} l_0^{\beta}} \cdot \left(\frac{l_0}{l_1} \right)^{(\alpha + \beta \gamma_1)/\gamma_1} \right) \frac{1}{\tilde{k}^{\gamma_1}} \tilde{P}_{l|k} \left(\frac{l_0}{\tilde{k}^{\gamma_1}} \right) P_k(\tilde{k}) d\tilde{k} \right] \\ &\quad + \int_0^{\theta_k (l_1/l_0)^{1/\gamma_1}} \frac{1}{k^{\alpha} l_1^{\beta}} \tilde{P}_{s|k,l} \left(\frac{s}{k^{\alpha} l_1^{\beta}} \right) \frac{1}{k^{\gamma_1}} \tilde{P}_{l|k} \left(\frac{l}{k^{\gamma_1}} \right) P_k(k) dk. \end{aligned}$$

One can easily show that the two integral terms in this strict relationship becomes negligible when $s \rightarrow \infty$. Under an additional condition that Eq. (S3.4) holds with $-\delta_l = -1 - (\delta_k - 1)/\gamma_1$,

$$P(s|l = l_1) = \frac{P(l = l_1, s)}{P(l = l_1)} \sim \frac{1}{l_1^{(\alpha + \beta \gamma_1)/\gamma_1}} \tilde{P}_{s|l} \left(\frac{s}{l_1^{(\alpha + \beta \gamma_1)/\gamma_1}} \right)$$

at $l_1 \rightarrow \infty$ and $s/l_1^{(\alpha + \beta \gamma_1)/\gamma_1} \rightarrow \infty$, where

$$\tilde{P}_{s|l}(\tilde{s}) = l_0^{(\alpha + \beta \gamma_1)/\gamma_1} \cdot P(l = l_0, s = l_0^{(\alpha + \beta \gamma_1)/\gamma_1} \cdot \tilde{s}).$$

Therefore, comparing this result with Eq. (S2.3), we have

$$\gamma_3 = \frac{\alpha + \beta \gamma_1}{\gamma_1}, \tag{S3.10}$$

for the upper tail of s in a limited condition.

Supplementary Text 4: Estimating Scaling Exponents

Here, we discuss the methods and results of our estimation of the scaling exponents in detail. First, we consider the rationales behind the estimations. Second, we check the consistency between the estimated scaling exponents with the mathematical relationships examined in Supplementary Text 3, in order to determine the thresholds that are used in the estimations. Third, we investigate the subtle changes of the scaling exponents with year and their relationships with GDP.

We first begin with the bivariate scaling relationships, formulated with Eqs. (S2.1–3) or (S3.1) and confirmed to be present in our data:

$$P(x|y) = \tilde{P}_{x|y}(x/y^\gamma)/y^\gamma,$$

where $P(x|y)$ is the probability density of x conditional on y , $\tilde{P}_{x|y}$ is a probability density function and γ is a positive constant. When a variable \tilde{x} is defined as $\tilde{x} \equiv x/y^\gamma$, we have

$$P(\tilde{x}|y) = \tilde{P}_{x|y}(\tilde{x}),$$

given that the probability density should satisfy the normalization $\int P(\tilde{x}|y) d\tilde{x} = 1$. The variable \tilde{x} does not depend on the y -value and, thus, \tilde{x} is independent of y .

This means that the exponent γ could be estimated by finding the optimal value that makes the \tilde{x} and y the most independent of each other. One of the simplest indexes for measuring the dependence between stochastic variables is the Pearson's product-moment correlation coefficient. Therefore, we obtain $\hat{\gamma}$, the estimated value of γ , by

$$\hat{\gamma} = \arg \min_{\gamma} \left(\text{Cor} \left[\log \left(\frac{x}{y^\gamma} \right), \log y \right] \right)^2. \quad (\text{S4.1})$$

where $\text{Cor}[\cdot, \cdot]$ means the correlation coefficient of the two terms. We apply the log-transformation to the raw data because the distribution of x conditional on y is heavy-tailed as shown in Fig. S4d–f. A few extreme values out of such heavy-tailed distributions could have a relatively high impact on the correlation coefficient compared to those from normal or exponential distribution as shown in Table S1.

This amounts to the linear least squares regression of $\log x$ against $\log y$. Indeed, when the correlation coefficient is zero, so is the covariance, and if we apply the transformations $x \leftarrow x/\bar{x}$ and $y \leftarrow y/\bar{y}$ where \bar{x} and \bar{y} represent the geometric mean of x and y ,

$$(N - 1) \cdot \text{Cov} \left[\log \left(\frac{x}{y^\gamma} \right), \log y \right] \equiv \sum_i \log y_i \cdot (\log x_i - \gamma \log y_i) = 0$$

or

$$\sum_i \log x_i \cdot \log y_i = \gamma \sum_i (\log y_i)^2, \quad (\text{S4.2})$$

where $\text{Cov}[\cdot, \cdot]$ means the covariance of the two, N is the number of samples and x_i and y_i denotes the i -th sample of x or y . Meanwhile, when the residual sum of squares is minimized,

$$\frac{\partial}{\partial \gamma} \sum_i (\log x_i - \gamma \log y_i)^2 = 0,$$

which is also satisfied by Eq. (S4.2).

Similar considerations are valid for the estimation of exponents in multi-variate scaling. Assuming Eq. (3),

$$P(s|k, l) = \tilde{P}_{s|k,l}(s/k^\alpha l^\beta)/k^\alpha l^\beta,$$

and defining $\tilde{s} \equiv s/k^\alpha l^\beta$, $P(\tilde{s}|k, l) = \tilde{P}_{s|k,l}(\tilde{s})$ follows. Therefore, α and β could be estimated with

$$(\hat{\alpha}, \hat{\beta}) = \arg \min_{\alpha, \beta} \left[\left(\text{Cor} \left[\log \left(\frac{s}{k^\alpha l^\beta} \right), \log k \right] \right)^2 + \left(\text{Cor} \left[\log \left(\frac{s}{k^\alpha l^\beta} \right), \log l \right] \right)^2 \right]. \quad (\text{S4.3})$$

When the correlations are zero so that the right hand side of Eq. (S4.3) is minimal, and when we apply the transformations $s \leftarrow s/\bar{s}$, $k \leftarrow k/\bar{k}$ and $l \leftarrow l/\bar{l}$, where \bar{x} denotes the geometric mean of a variable x ,

$$\sum_i (\log s_i - \alpha \log k_i - \beta \log l_i) \cdot \log k_i = \sum_i (\log s_i - \alpha \log k_i - \beta \log l_i) \cdot \log l_i = 0,$$

where k_i , l_i and s_i denotes the i -th sample of k , l or s . In this condition, we can see that

$$\frac{\partial}{\partial \alpha} \sum_i (\log s_i - \alpha \log k_i - \beta \log l_i)^2 = 0; \quad \frac{\partial}{\partial \beta} \sum_i (\log s_i - \alpha \log k_i - \beta \log l_i)^2 = 0. \quad (\text{S4.4})$$

Therefore, the estimation in Eq. (S4.3) is equated to the linear least squares regression of $\log s$ against $\log k$ and $\log l$, without the interaction term.

Although it is more formal to orthogonalize explanatory variables in the regression analysis, the method presented above gives a result equivalent to the orthogonalized version. Let us consider the regression of $\log s$ against $\log k$ and $\log[l/k^{\gamma_1}]$, where γ_1 is a constant determined empirically ($\gamma_1 \sim 1.0$ as later shown in as shown in Fig. S5c). The variables are again normalized with the transformation $x \leftarrow x/\bar{x}$, where \bar{x} represents the geometric mean of a variable x . Here, the exponents, α' and β' , are intended to fulfill the multi-variate scaling $s \propto k^{\alpha'} (l/k^{\gamma_1})^{\beta'}$ and thus estimated as

$$(\hat{\alpha}', \hat{\beta}') = \arg \min_{\alpha', \beta'} \left[\text{Cor} \left[\log \left(\frac{s}{k^{\alpha'} (l/k^{\gamma_1})^{\beta'}} \right), \log k \right]^2 + \text{Cor} \left[\log \left(\frac{s}{k^{\alpha'} (l/k^{\gamma_1})^{\beta'}} \right), \log(l/k^{\gamma_1}) \right]^2 \right].$$

When the correlations are zero,

$$\sum_i (\log s_i - \alpha' \log k_i - \beta' (\log l_i - \gamma_1 \log k_i)) \cdot \log k_i = 0; \quad (\text{S4.5})$$

$$\sum_i (\log s_i - \alpha' \log k_i - \beta' (\log l_i - \gamma_1 \log k_i)) \cdot (\log l_i - \gamma_1 \log k_i) = 0. \quad (\text{S4.6})$$

Adding Eq. (S4.6) to Eq. (S4.5) multiplied by γ_1 , we have

$$\sum_i (\log s_i - \alpha' \log k_i - \beta' (\log l_i - \gamma_1 \log k_i)) \cdot \log l_i = 0. \quad (\text{S4.7})$$

Equations (S4.5) and (S4.7) is met with $\alpha' = \alpha + \beta\gamma_1$ and $\beta' = \beta$ when Eq. (S4.4) holds. Therefore, the estimated value of exponents in a formal regression analysis can be derived from the regression with the explanatory variables not orthogonalized. Note that α' is just the mathematically expected value of γ_2 as shown in Eq. (S3.9).

Although the linear regressions could give the estimations of scaling exponents in principle, we should consider what data to exclude from the analysis. This is because the scaling relations do not perfectly describe the data for all ranges of variables. For example, we can see some deviations from the scaling relations especially for the number of trading partners k and the employee number l less than 10 (Figs. 2a and S4a–c). Since firms of smaller size dominate the data (Fig. S2), their deviation from the scaling should heavily affect the estimation. Indeed, without any data exclusion from the compiled data, there is a considerable gap between the direct and indirect estimations of δ_l (the power-law exponent of l distribution). Whereas we see that $\delta_l \approx 2.2$ from Fig. S2b, $\delta_l \approx 2.7$ is expected from Eqs. (S3.4) and (S3.5), since $\gamma_1 \approx 0.75$ (Fig. S5a), $\delta_{l|k} \approx 2.7$ (Fig. S4d) and $\delta_k \approx 2.2$ (Fig. S2a). To ensure the consistency between the exponents, $\gamma_1 \approx 1.0$ should hold. Additionally, there is a clear difference between the expected value of γ_3 (dashed purple line) from Eq. (S3.10) and the value of direct estimation (solid purple line) as shown in Fig. S5a.

To obtain a consistent set of estimates that does not contradict the mathematical relations mentioned in Supplementary Text 3, we try two thresholds, 10 and 100. If the ‘explanatory’ variables in the right hand side in Eq. (2) or Eqs. (S2.4–6) take a value under the threshold, we neglect the datum. The results are shown in Fig. S5b for the threshold 10 and 5c for 100. We see that γ_1 nearly becomes 1.0 and the direct and indirect estimates of γ_3 agree to each other only when the threshold is set at 100. This suggests that the threshold should be no less than 100 for k and l . For the sake of sample size, we employ the threshold value of 100. The sample sizes before and after the threshold is applied are shown in Fig. S5d.

We determine the scaling exponents for every year to assure the stability of our results. Yearly estimation of the exponents is shown in Fig. S5c. The slow fluctuations of estimated α (black line) and β (red line) are noticeable. However, we need an uncertainty measure to judge whether the fluctuations are meaningful.

Despite our use of linear regression, the estimation of uncertainty needs a nonparametric method, since the ‘error terms’ (Fig. S4d–f) are not normally distributed. To this end, we perform the bootstrap method [7] to get the CI (confidence intervals). Resampling is done 10,000 times and the resampling size is identical to the sample size. The 95% confidence intervals are determined as the 2.5- and 97.5-percentiles of the bootstrap distribution.

Although the changes are not radical and the inequality $\alpha < \beta$ is invariably met, as shown in Fig. 4, The exponents α and β become smaller and larger respectively in the 2000–2005 period compared to the 2013–2015 period. The difference is ‘significant’ in the loose sense that the 95% confidence intervals are not overlapping. It is also clear that α and β are negatively correlated, which is expected from Eq. (S3.9) and relatively constant γ_1 and γ_2 (Fig. S5c). This implies that the only variants in the system at this level of coarse-grained observation are the values of α and β , considering the relative invariability of γ_1 , γ_2 and γ_3 and distributional functions (Figs. 2f and S5c).

It is intriguing to see that α and β respectively seem counter- and pro-cyclical: i.e. it is apparently positively or negatively correlated to the nominal GDP of the country [8], as indicated in Figs. S6a and S6b. GDP is selected here because its cycle of fluctuation is longer compared to other indices of the economic climate, such

as Indexes of Business Conditions reported by Cabinet Office, Government of Japan [9]. A closer inspection reveals that α is enlarged when the nominal GDP decreases (Fig. S6a) and that β goes down almost simultaneously with GDP while its increase is delayed with respect to GDP expansion (Fig. S6b). However, we could not rule out the possibility that this is a mere coincidence, since the dataset covers only slightly more than one cycle. Considering the fact that the cycle is about twenty years long, it might need one more decade or a dataset from another country to verify this trend.

We furthermore calculate the cross-correlation between GDP and the exponents to evaluate the delay quantitatively. The normalized cross correlation $CC_\tau[x, y]$ is here defined by the Pearson's correlation coefficient applied to lagged time-series data $x(t)$ and $y(t + \tau)$ defined for discrete time $t_0 \leq t (\in \mathbb{Z}) \leq t_{\text{end}}$:

$$CC_\tau[x, y] \equiv \frac{1}{N-1} \sum_{T_\tau} \tilde{x}(t) \tilde{y}(t + \tau) / \sqrt{\frac{1}{N-1} \sum_{T_\tau} \tilde{x}(t)^2} \sqrt{\frac{1}{N-1} \sum_{T_\tau} \tilde{y}(t + \tau)^2},$$

where $T_\tau \equiv \{t \in \mathbb{Z} \mid t_0 + \tau \leq t \leq t_{\text{end}} + \tau\}$, N is the length of the time-series (i.e. the number of elements in the truncated set T_τ) and

$$\tilde{x}(t) \equiv y(t) - \frac{1}{N} \sum_{T_\tau} y(t) \quad \text{and} \quad \tilde{y}(t) \equiv y(t) - \frac{1}{N} \sum_{T_\tau} y(t).$$

We plot $CC_\tau[\text{GDP}, \hat{\alpha}]$ and $CC_\tau[\text{GDP}, \hat{\beta}]$ against τ in Fig. S6c, and see that both peaks at $\tau = 1$ (negatively and positively, respectively), with Pearson correlation coefficient as high as -0.59 and 0.58 . To add, the second highest peak is present in both cross correlation series, probably reflecting the fact that the extent of delay in exponent changes is different for GDP increase and decrease. Note that the reversal of sign at τ value far from 0 is the artefact of the time window that covers only slightly more than one economic cycle. The result suggests that the scaling exponents are affected by GDP of the previous year on average. We suspect that some parameters in inter-firm trades are mechanistically affected by GDP. However, we have no further support for this statement at the present study.

Supplementary Text 5: Generality of Growth Correlations

In this note, we assess the generality of the results represented in Fig. 5 for firms of different sizes. Fig. 5 shows that Group 2 firms (with an employee growth by a factor over 1.5) outperform Group 1 firms (with a trading partnership growth by a factor over 1.5) in sales growth on average when the size vector in the initial year is controlled for. However, in the main text, we only examine the case of the number of trading partners $k \sim 10$. Here we check the validity of our claim in other cases.

We first compare Group 2 against Group 1 for different sets of firms on the scaling line (Fig. 3a) with the same setup as in the main text. More specifically, the following procedures are applied to our data. First, a point on the scaling line is determined from a value of k , ranging from 10^0 to 10^4 , with Eq. (S6.1). Firms' Euclidean distance d_{\log} from this point in log-transformed scales (Eq. (5)) is used to obtain a set of firms that are

located closely around the point (i.e. $d_{\log} < \log[10^{1/8}]$) in the initial year $t-1$. The firms are searched over the entire data, but the initial year ranges from 1994 only to 2013 so that we can trace the sales change in the following year $t+1$. If the sample size does not reach 1,000, the threshold of d_{\log} is enlarged until there are equal to or more than 1,000 samples. Then, we determine three mutually exclusive sets of firms from these samples, namely (i) ‘Control’ firms whose yearly changes in both the number of trading partners k and employee number l are within $\pm 20\%$, (ii) ‘Group 1’ firms which increase the number of trading partners k by over a factor of 1.5 in a year but keep their change in employee number l within $\pm 20\%$ and (iii) ‘Group 2’ firms which grow in l by over a factor of 1.5 in a year but keep their k change within $\pm 20\%$ in the same period. This ensures that the correlation between g_k (annual k growth) and g_l (annual l growth), which is already weak (SFig. S8), does not affect the difference between these groups. Averages of the log-transformed sales growth in the same year ($\log[s(t)/s(t-1)]$) and in the following year ($\log[s(t+1)/s(t)]$) are calculated for each group of firms, and the uncertainty of the value is indicated by the 95% confidence interval determined by the bootstrap method [7], where 2.5- and 97.5-percentiles in the resampling distribution is obtained from 10,000 resamplings.

It is evident that the average sales growth of Group 2 firms is higher compared to that of Group 1 firms when the firm size in the number of trading partners k is smaller than 30, as is shown in Fig. S7a and b. This is true both for the ‘coinciding’ sales growth in the year t (Fig. S7a) and for the ‘following’ one in the year $t+1$ (Fig. S7b). Additionally, the average growth of Group 1 or Group 2 firms is almost always above the level of Control firms, suggesting that the growth either in k or in l has a positive effect on the sales growth.

However, the difference between Group 1 and 2 is hard to see for larger firms, largely because of the fewer sample sizes. Also note that the size fluctuation is smaller for larger firms [4,10–13], and the larger the firm is, the rarer is the ratio of firms that experience a size growth higher than 50%. The weak but higher correlation between k and l growth in large firms compared to the small firms (Fig. S8) further reduces the number of firms included in the high-growth groups.

To address this problem, we also relax the definition of Group 1 and 2, allowing firms which grow in k or l by over a factor of 1.2 (instead of 1.5) to enter the groups. The results are shown in Fig. S7c and d. They also support the difference of sales growth between the two groups when the initial k of the firms is smaller than 30, but it seems that growth in the number of trading partners sometimes has more positive effect on sales growth in the same year compared to employee growth when the initial k is larger than 100. It is hard to conclude, however, as again the sample size is still small. For example, even in this setting, we have only 14 and 13 firms for Group 1 and 2 when the initial firm size is set to be $k \sim 10^3$. Also note that a high risk of false positives is present, where a significant effect is detected from the sample data although no such effect exist in experimental situations, since multiple comparisons are performed here for sets of firms of different sizes.

To sum, Group 2 firms (with a large employee growth) has higher sales growth compared to Group 1 firms (with a large growth in the number of trading partners), at least when the firms are small- or medium-sized ($k < 30$). Group 1 and Group 2 firms are both likely to outperform Control firms with small changes in employee size or trading partnership. However, it is unclear whether Group 2 always attain higher sales growth on average

compared to Group 1 when the firms are large.

Supplementary Text 6: Evolutionary Flow Diagram

This note provides a detailed explanation of the methods and results regarding the evolutionary flow diagrams. First, we explain how to determine the absolute position of the ‘scaling line’ shown in the diagrams. Second, we describe the methodology whereby we render streamlines indicating the flow. Third, we describe the results in more detail than in the main text, showing slices covering entire ranges of the 3-dimensional vector space.

We define the ‘scaling line’ in accordance with Eqs. (2) and (S2.4). Taking the median of their right hand side, we have

$$\log l = \gamma_1 \log k + \langle \varepsilon_{l|k} \rangle_{0.5} \quad \text{and} \quad \log s = \alpha \log k + \beta \log l + \langle \varepsilon_{s|k,l} \rangle_{0.5}, \quad (\text{S6.1})$$

which can be interpreted as planes in the 3-dimensional space. We regard the line of intersection of these planes as the central line of scaling. Although the line should be determined only from the bivariate scaling relations in principle, there would be difficulty since there does not always exist a 3-dimensional line such that different lines on three different planes are just the projections of the 3-d line to the planes. We use the median rather than with the average here, because the distribution of l conditional on k , $\tilde{P}_{l|k}$ (Fig. S4d), or of s conditional on both k and l , $\tilde{P}_{s|k,l}$ (Fig. 2b) is heavy-tailed and the average does not give an intuitive representative value. We thus compute the medians of $\log l - \gamma_1 \log k$ and $\log s - \alpha \log k - \beta \log l$ as the intercept of the planes, where the sample of k (for the former) or both k and l (for the latter) is confined above the threshold 100. The values of α , β and γ_1 used in the calculation are estimated in the same way as in Methods section, except that the source data are aggregated regardless of the year.

We rendered the streamlines in Figs. 6 and S9, exploiting the method developed elsewhere [14] in order to render a 2-dimensional diagram which is visibly easy to interpret. In summary, it follows two steps: (i) placing some points randomly on the plane and drawing streamlines that pass through them, and (ii) repeatedly comparing the original image with a randomly modified one and selecting the one in which the streamlines are placed more homogeneously. Random modifications include inserting, deleting, lengthening, shortening and (almost) parallel moving of a streamline and combining of two. The measure of homogeneity for a set of placed streamlines is defined with a blurred image of them.

We render the individual streamlines by the 4th order Runge-Kutta method. For the purpose of reducing the computational power required, we apply the transformation below to the original vector field:

$$\mathbf{g}(k, l, s) \leftarrow \frac{\mathbf{g}(k, l, s)}{|\mathbf{g}(k, l, s)|^c},$$

where $\mathbf{g}(k, l, s)$ in the right hand side represents the 3-dimensional vector of average log-transformed growths at a point in the vector space, estimated as in Methods section, and $0 < c < 1$ the degree of ‘acceleration’. In this transformation, the streamlines ideally remain the same, since the direction in which an average firm of the size vector proceeds does not change at any point. It, however, accelerates the iteration when the speed is nearly

0, thus drastically reduces the computational needs. We set $c = 0.7$, considering the trade-off between the computational power reduced and precision of the drawing near the equilibrium point.

Some minor adjustments applies to the method. One is the omission of re-calculation of streamlines. In the original method, one should render the streamlines from scratch every time the modification is performed. This is not computationally feasible in our case, due to the fact that the drawing of a streamline need a substantial computational power. To apply the original methodology of streamline selection in this situation, we obtain 400 lines in advance and assign numbers to them such that a line to which a number is assigned is closer to the lines of the adjacent numbers than to other ones. Another adjustment in the algorithm is that the random combining is not allowed here. This serves to avoid combining streamlines of different orientations.

We exhibit all the resulting evolutionary flow diagrams for a variety of slicing planes in Fig. S9. The vector space is sliced with planes of a constant k (trading partners number) that ranges from 1 to 10^4 in Fig. S9a–e; a constant l (employees number) that ranges from 1 to 10^4 in 8f–j; a constant s (annual sales in million yen) that ranges from 1 to 10^6 in 8k–q.

We notice several remarkable aspects. The first one is that firms generally flow towards the scaling surface (see Fig. 2a for data of year 2014 and Fig. 6 for aggregated data). The contours indicating the surface are marked by yellow lines in the figures. Although the sales growth is not exactly zero at all the points in the scaling surface, this might well occur as a result of stochasticity and uncertainty. The fact lends credibility to the observation, that the trend of near-zero growth on the scaling surface is more obvious at the center of yellow contours and at medium s -levels than elsewhere, as the sample density is larger in these zones.

Secondly, we note the ubiquitous flow toward the scaling (red) point for slice with l in Fig. S9f–j or with s in Fig. S9k–q. Additionally, the speed of flow is almost zero around the red point, indicating the fact that firms hardly move on average once they reach this point. It follows that the scaling line is an attractor if we regard the system as a dynamical system, where the firm development is determined only by the average flow and has no stochasticity. Note that this might not be the case for the largest firms: firms with the highest number of employees l ($> 10^4$) with $k > 10^3$ and $s > 10^5$ tend to decrease their employees, and seem more stable at a smaller l . If this is true, it might be related to the seeming plateau of s at the highest l (Fig. S4c). However, the degree for which this is true is a matter of question, as the estimates of growth rates would be inaccurate there.

Third, as visible in slices with a constant sales s in Fig. S9k–q, increasing of trading partners does not have so positive effect on the sales growth rate as the employee increase. It even negatively affect the sales growth when sales is low (Fig. S9k and l).

We also show contour plots of firm exit rates for a variety of slicing planes in Fig. S10. The space is sliced with the same planes as in Fig. S9. We can see two phases in the figures. First, when the firms are over the medium size (i.e. $k \geq 10$, $l \geq 10$ or $s \geq 10^3$), the exit rate is generally higher at locations far from the scaling (red) point than at the vicinity of it, although it is not homogeneously high. In contrast, in the case where the sales is very low (i.e. $s < 10^2$, Fig. S10k and l), where no k or l value larger than 1 is possibly on scaling, lower exit rate coincides with more trading partners k and less employees l . Note that the placement of background colors in Fig.

S10k and l are similar to that in Fig. 9k and l. This suggest that the two phases mentioned in this paragraph also regulate some aspects of growth rates.

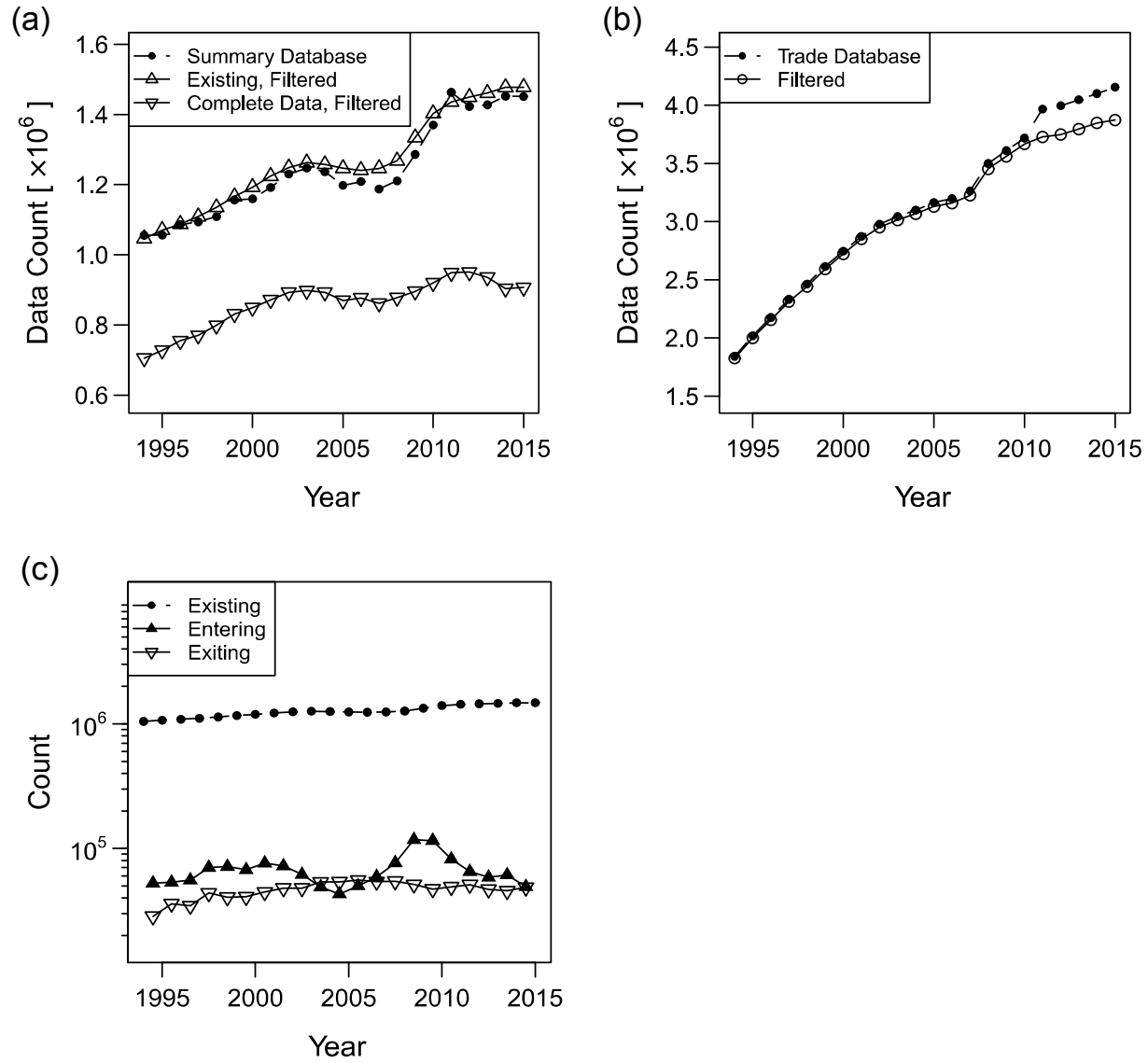


Figure S1. Change of data amount through the period 1994–2015. (a) The data amount of the original summary database (dashed line and black dots), number of existing firms after the filtering and integration with network data (upward triangle) and firms with data of all the three variables (downward triangle). (b) The data amount (number of links) of the original trade database (dots) and the after the filtering (circles). (c) The number of appearing (upward triangle) and disappearing (downward triangle) firms. The number of existing firms (dots) are plotted for the sake of comparison. Note that the vertical axis is in logarithmic scale.

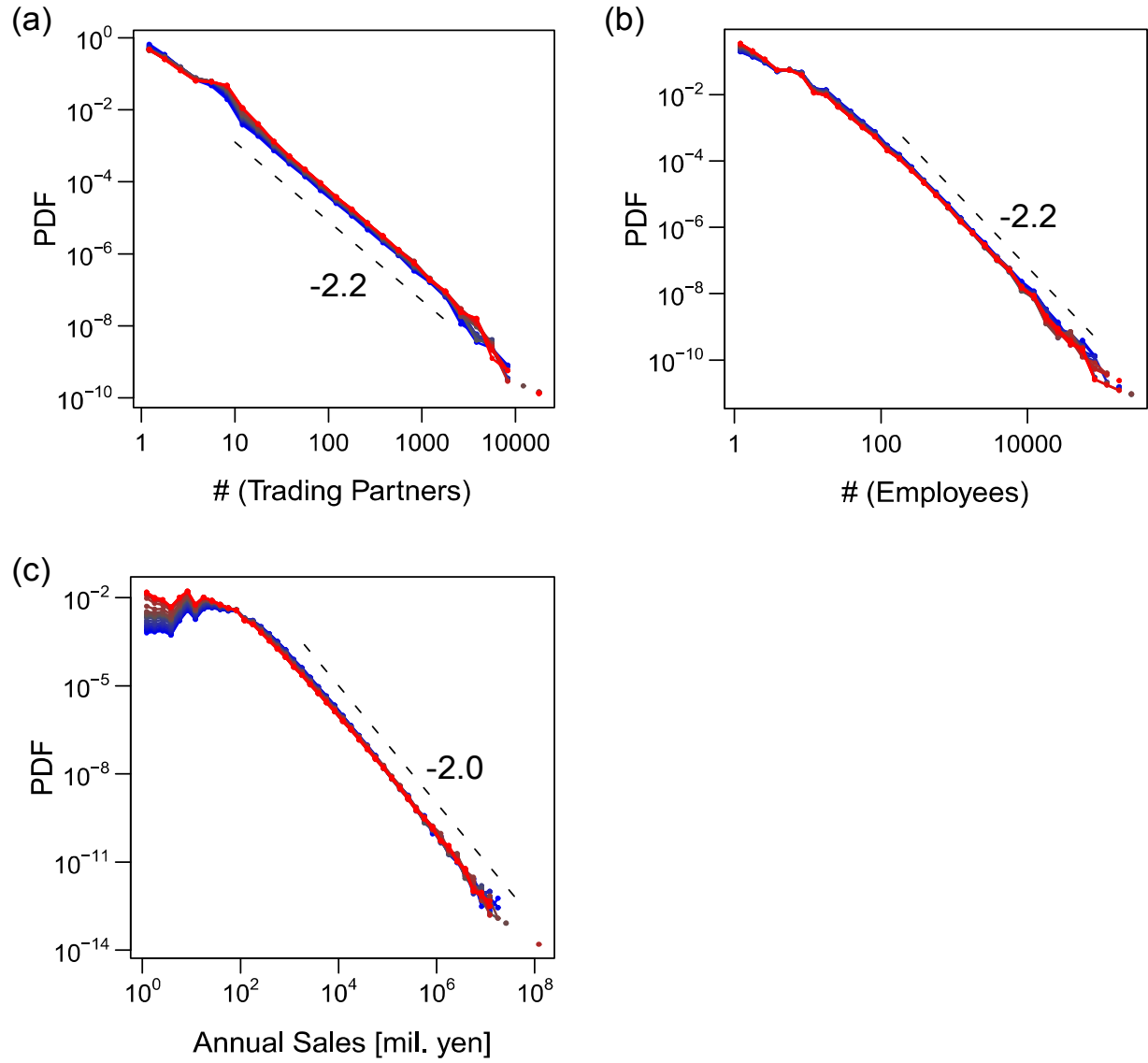


Figure S2. Probability distribution function (PDF) of the size variables through the period 1994-2015. The figures are plotted in log-log scales. Blue to red gradient of the color indicate the direction from old to new data. (a) Trading partners number. (b) Employee number. (c) Annual sales in million yen.

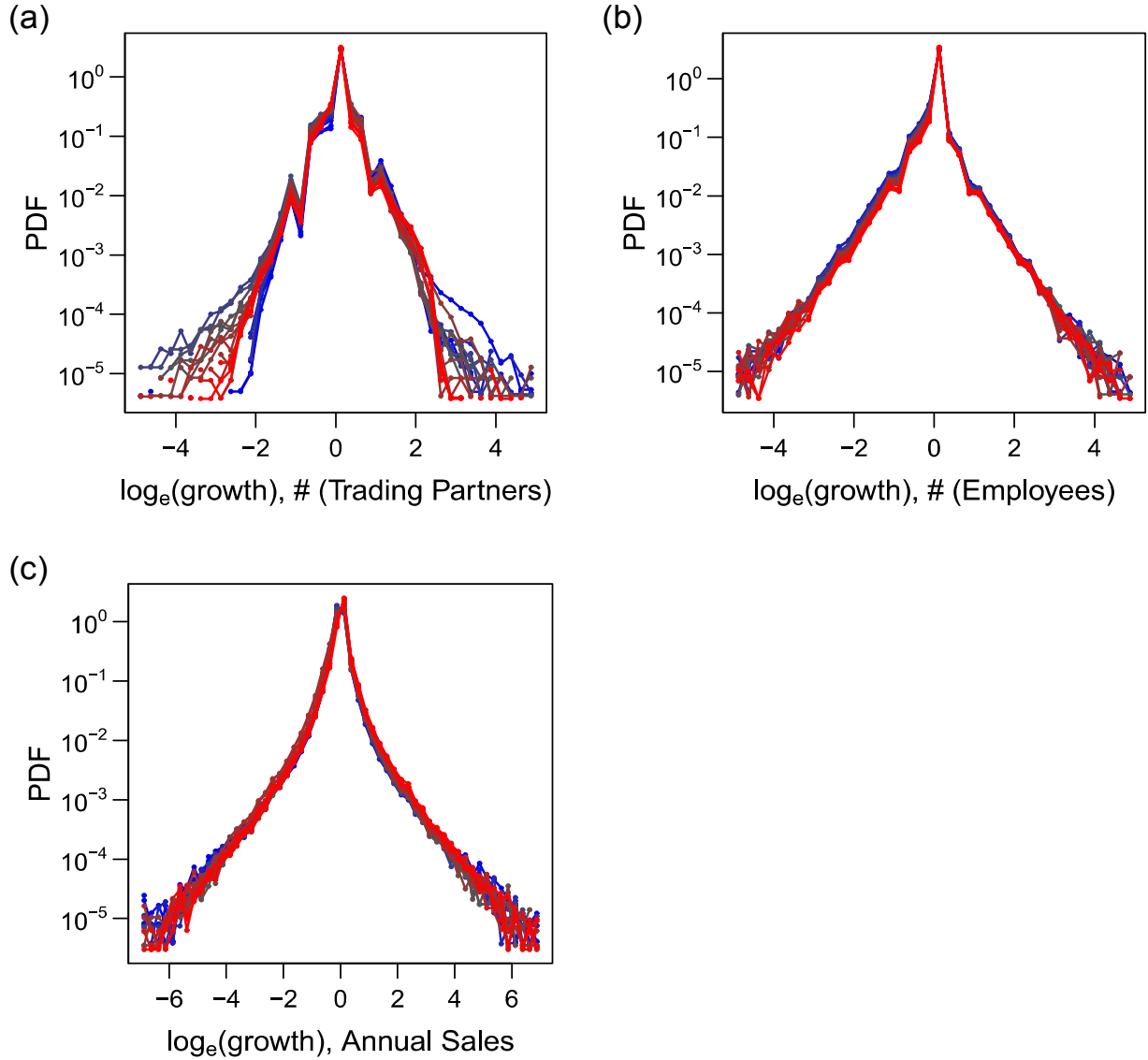


Figure S3. Probability distribution function (PDF) of the growth rate of size variables transformed by natural logarithm through the period 1994–2015. Growth rate is defined as the ratio of a value at a given year to that at the previous year. The distribution is not conditional on another variable. Note that the vertical axis is plotted in logarithmic scale. Blue to red gradient of the color indicate the direction from old to new data. **(a)** Growth rate of trading partners number. The zigzagged form at the center is due to the fact that the number of trading partners are integer, and a very large fraction of firms has only a few trading partners (Fig. S2a). **(b)** Growth rate of employee number. **(c)** Growth rate of annual sales in million yen.

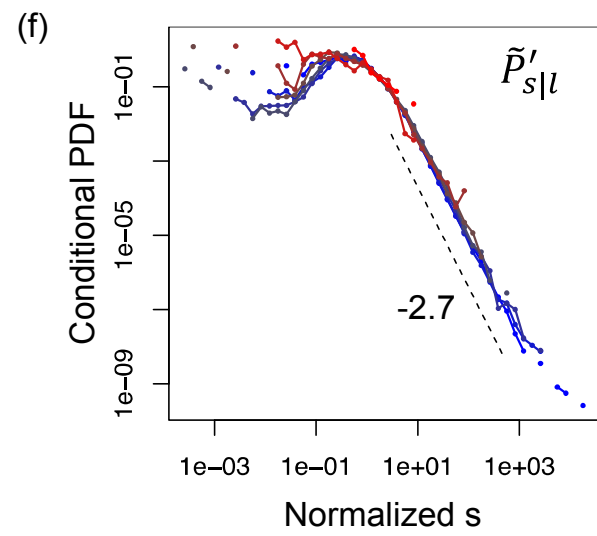
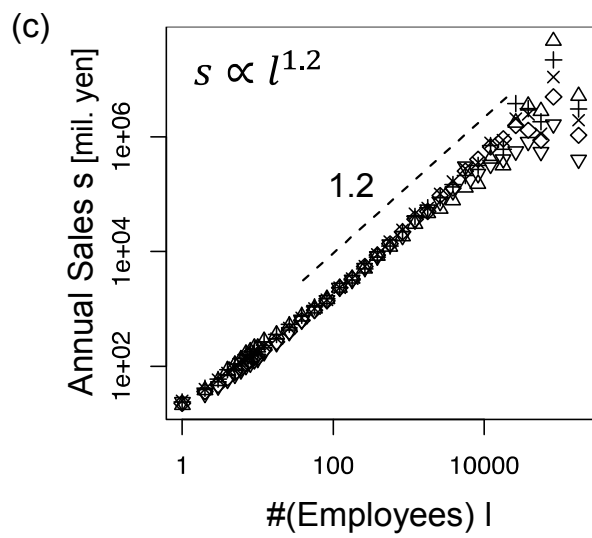
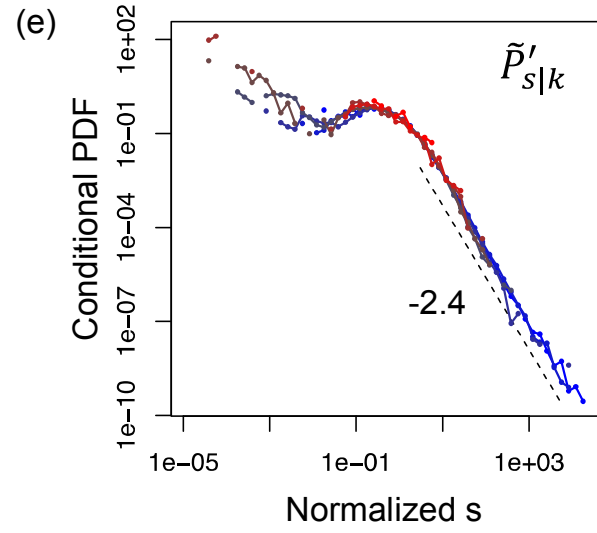
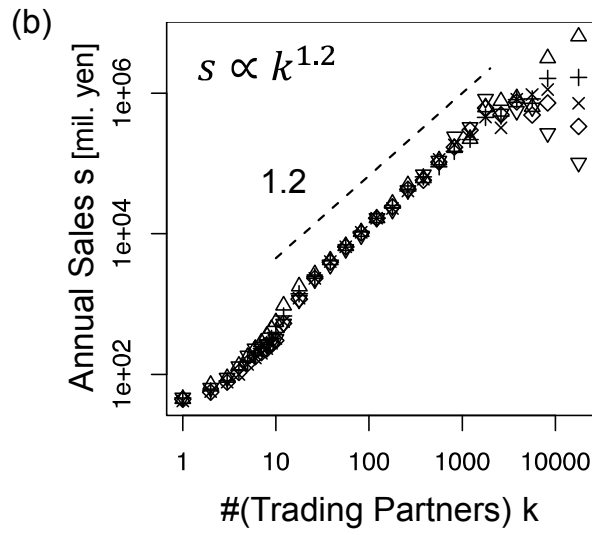
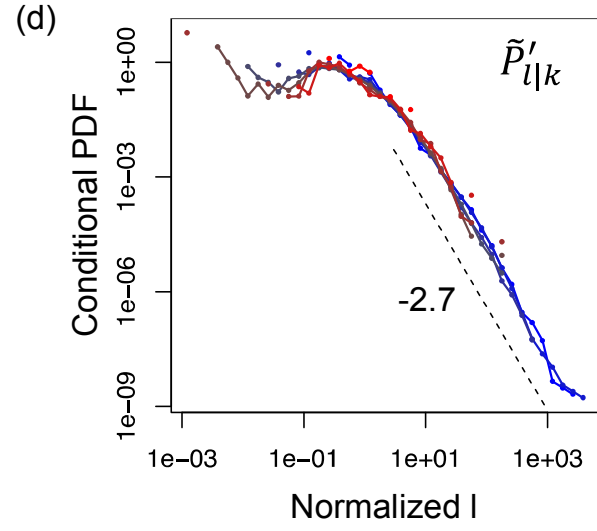
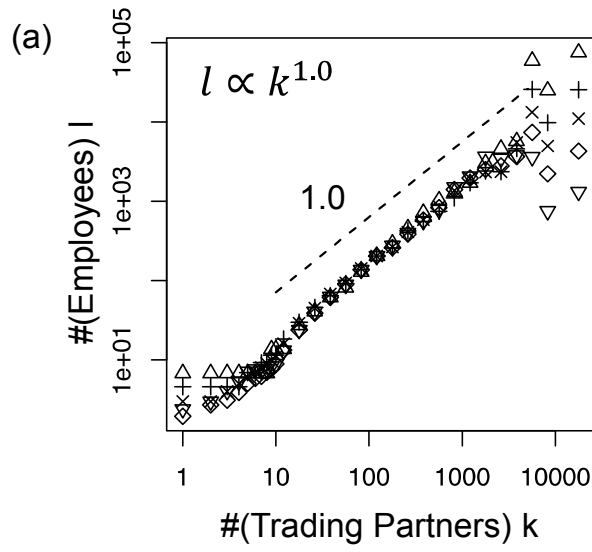


Figure S4. Scaling relations between pairs of size variables. The variables are the number of trading partners k , the number of employees l and annual sales in million yen s . All the data used in the figures are for 2014. **(a–c)** The 0.95(∇), 0.75(+), 0.5(\times), 0.25(\diamond) and 0.05(\triangle) quantiles of conditional distribution of l or s (vertical axis) are plotted against another variable k or l (horizontal axis) in a log-log scale. The variable of horizontal axis is divided into intervals of identical lengths in log scale (6 segments per a 10-fold interval) for k and $l > 10$ and of a unity in linear scale for k and $l \leq 10$. Quantiles other than those of $q = 0.5$ (i.e. medians) are plotted with horizontal shift, so that all the curves pass through a point whose x -axis is slightly more than 100. **(d–f)** The probability distributions (PDF) of l or s conditional on k or l (namely, $P(l|k)$, $P(s|k)$ and $P(s|l)$), normalized by their conditional medians, are plotted in log-log scale. Conditional distributions are obtained for intervals of the ‘explanatory’ variable (k or l), where the entire range (a unity to the maximum of the variable) is evenly divided logarithmically into 8 segments. Color gradient of blue to red of the points and curves indicates low to high values of the ‘explanatory’ variable.

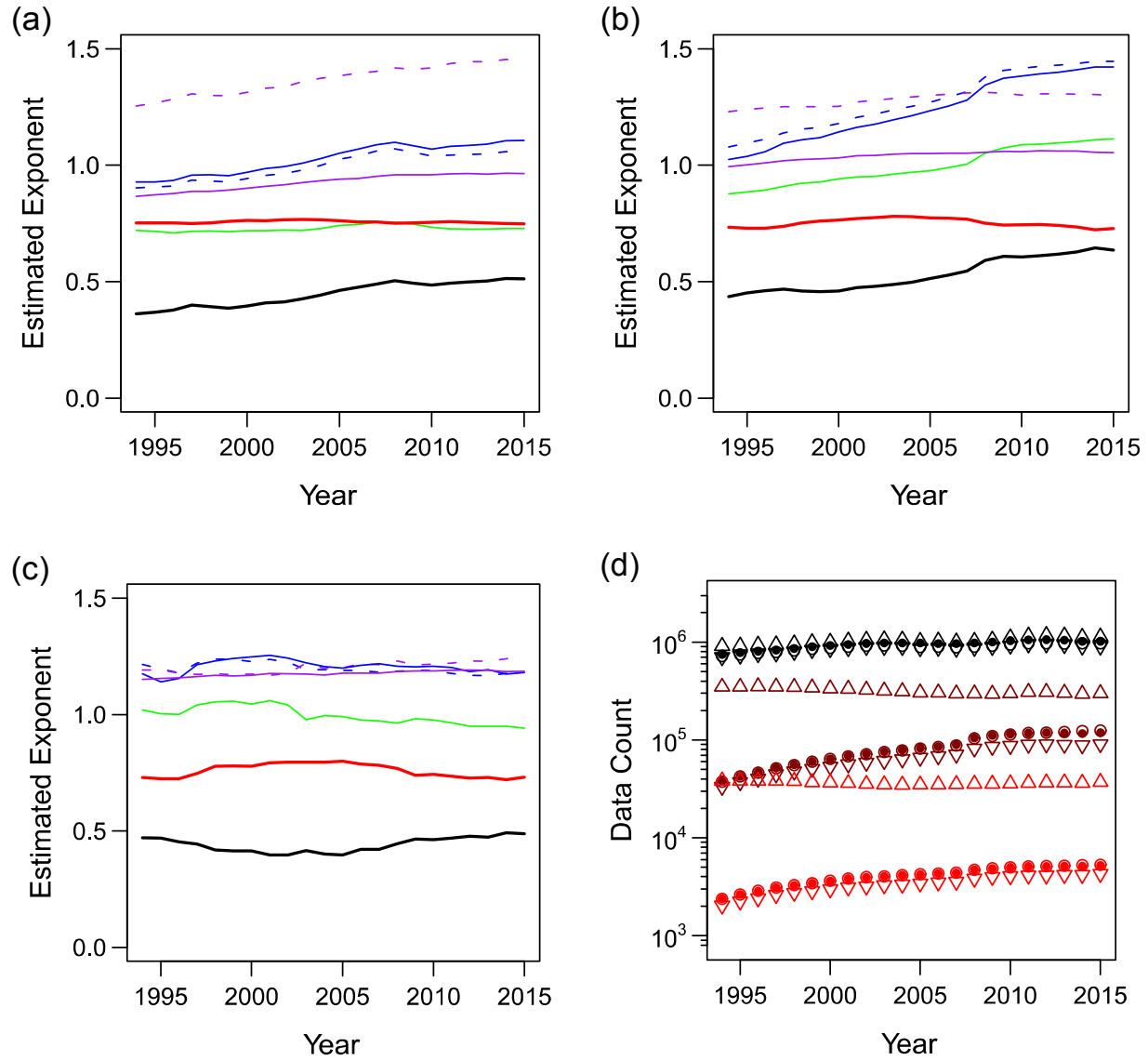
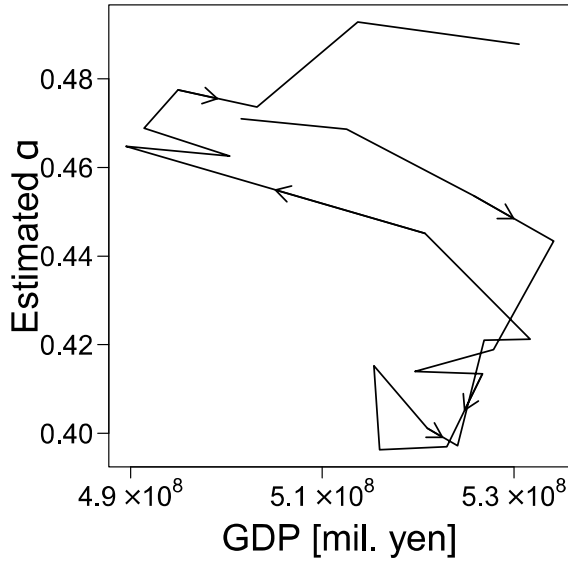
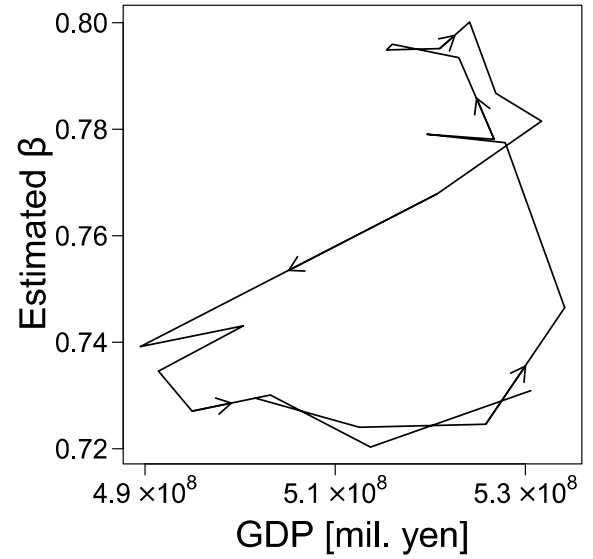


Figure S5. Estimated exponents of the scaling relationships through the period 1994–2015. The exponents of $l \propto k^{\gamma_1}$ (green), $s \propto k^{\gamma_2}$ (blue), $s \propto l^{\gamma_3}$ (purple) and α (black) and β (red) in $s \propto k^\alpha l^\beta$ are plotted. Additionally, the expected value of γ_2 and γ_3 derived mathematically from α , β and γ_1 in case of perfect scaling (Supplementary Text 2, Eqs. (S2.9) and (S2.10)) are juxtaposed (dashed line in blue and purple). **(a)** All the available data is used to estimate the exponents. **(b)** Used only the data where the ‘explanatory’ variable is larger than 10. **(c)** Used only the data where the ‘explanatory’ variable is larger than 100. **(d)** Plot of the size of samples from which the exponents are estimated against the year. Black, brown and red points indicate the threshold 0 (no exclusion), 10 and 100, corresponding to panel (a), (b) and (c). Hollow (\circ) and filled (\bullet) circles, upward (\triangle) and downward (∇) triangles respectively represent the scaling of l vs. k , s vs. k , s vs. l and s vs. l .

(a) GDP vs estimated α



(b) GDP vs estimated β



(c) Cross Correlation

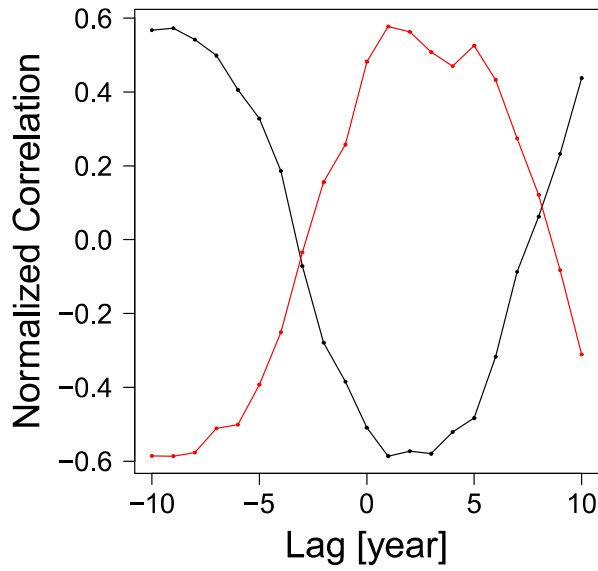


Figure S6. Estimated exponents α (for the number of trading partners k) and β (for the number of employees l) with the country's nominal GDP for different years in 1994–2015. The arrows indicate the time evolution. (a) The estimated α against the GDP. (b) The estimated β against the GDP. (c) Cross correlations between Nominal GDP and α or β are plotted against the time lag.

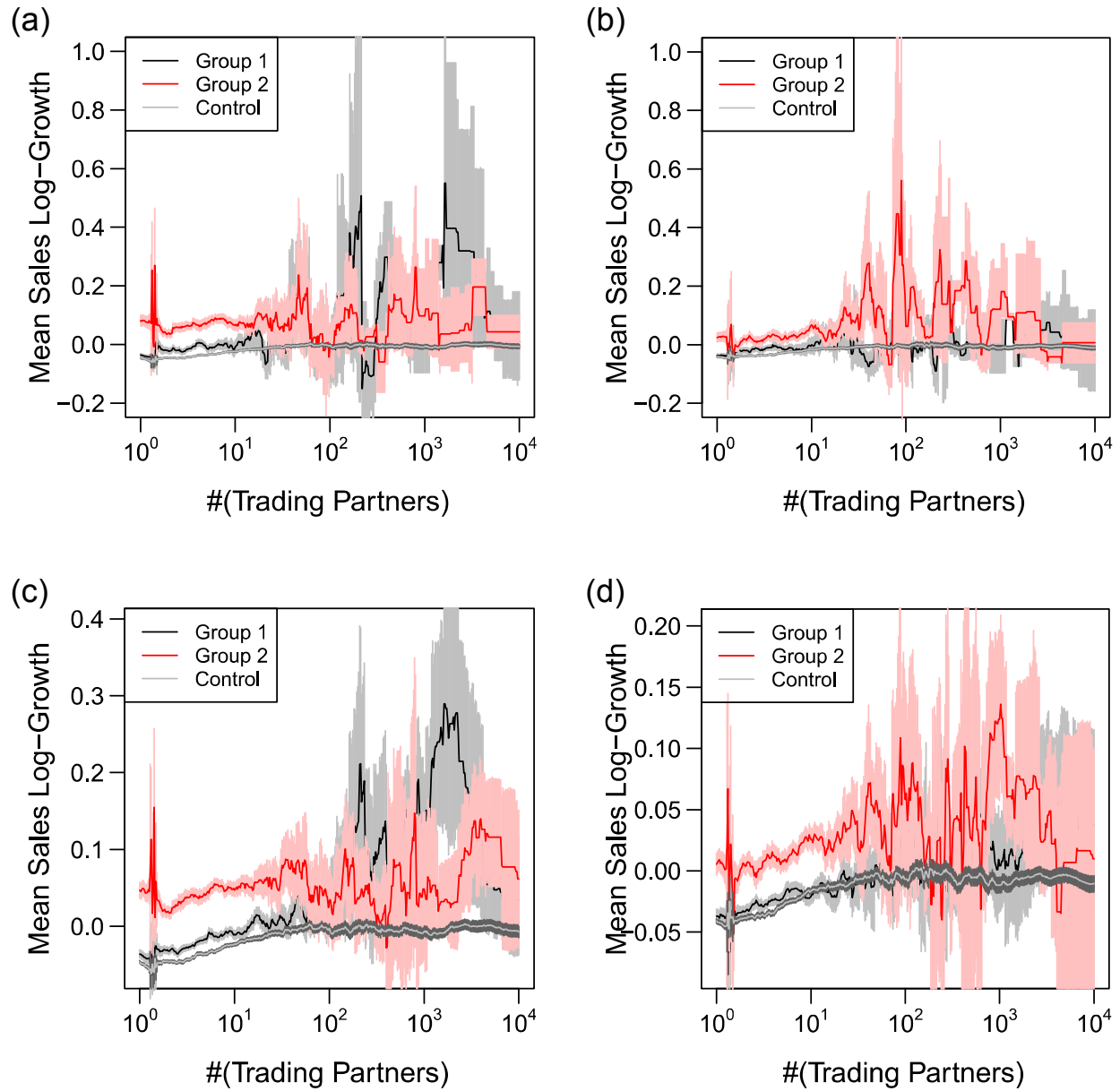


Figure S7. Average log-transformed growth rate of firms in Group 1 (black), Group 2 (red) and Control group (light grey) against the initial firm size. The colors around the line (grey for Group 1, pink for Group 2 and dark grey for Control) indicate 95% confidence intervals. The firm are sampled from around the scaling line. **(a–b)** Plot of average log-transformed sales growth of the same year (panel (a)) or the following year (panel (b)) against the firm size. Firms are included into Group 1 or 2 by over 50% growth in the number of trading partners or in employee number. **(c–d)** Plot of average log-transformed sales growth of the same year (panel (c)) or the following year (panel (d)) against the firm size. Firms are included into Group 1 or 2 by over 20% growth in the number of trading partners or in employee number.

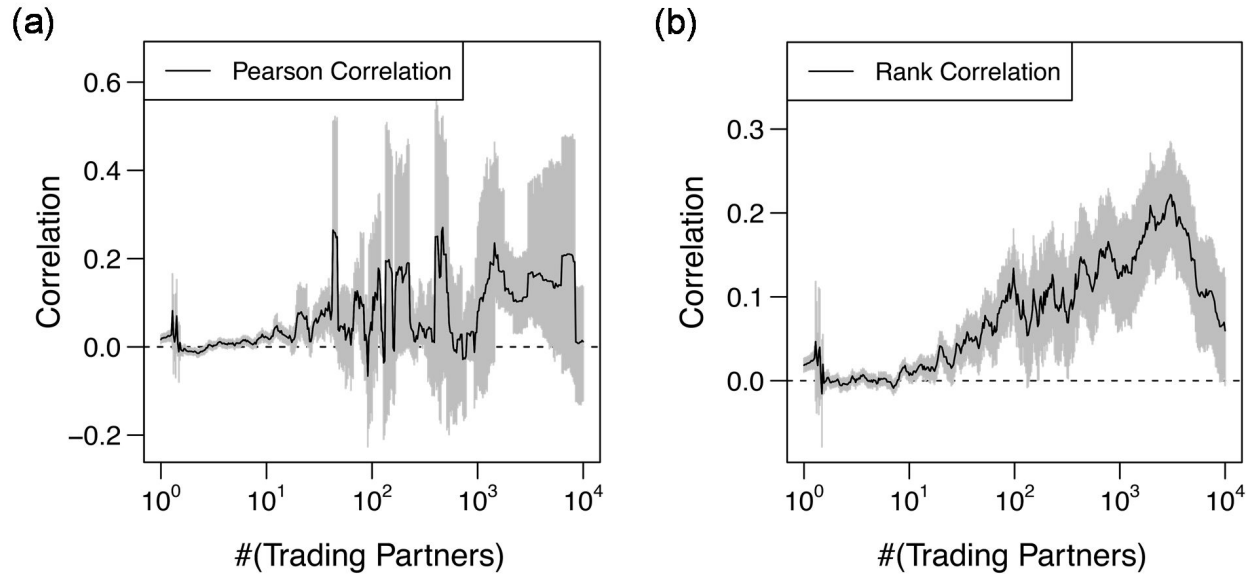


Figure S8. Correlation coefficients between annual growth in trading partners and employees. The central black curve is the estimated, while the grey bandwidth indicates the 95% confidence interval calculated by the bootstrapping method with 10,000 resamplings. **(a)** Plot of the Pearson correlation coefficient between the growth rates of employees and trading partners against the firm size. **(b)** Plot of the Spearman's rank correlation coefficient between the growth rates of employees and trading partners against the firm size.

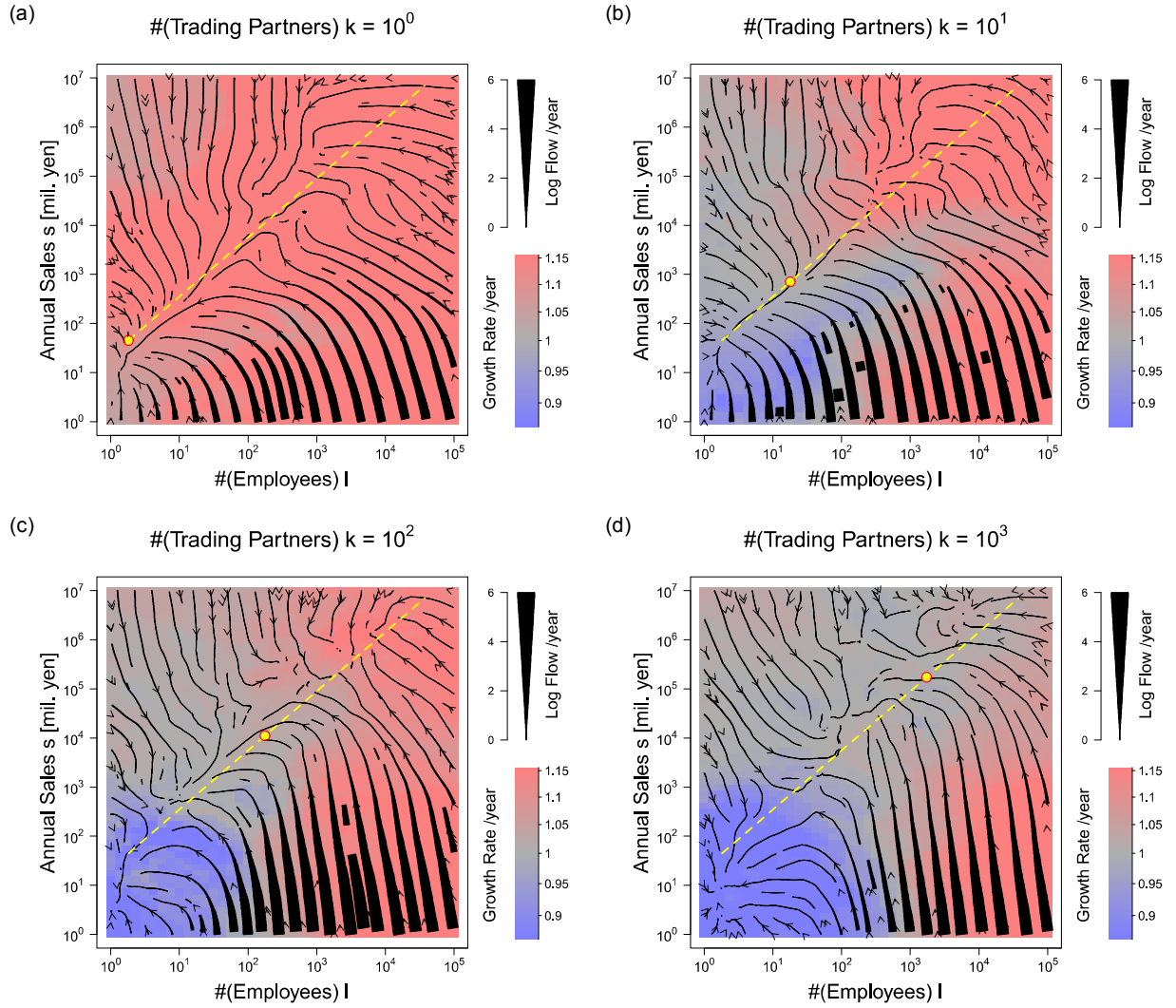


Figure S9. Evolutionary Flow Diagram, which illustrates estimated average log-transformed growth per year in the slice of the vector space. The direction and width of the black curves drawn indicate the velocity vector of average flow in the slicing plane. The estimated average flow orthogonal to the plane is illustrated with a background color, red, grey or blue representing plus, zero or minus growth. The yellow dashed line indicates the orthogonal projection of the scaling line to the "slicing plane" and the yellow and red point on the line represents the intersection point of the slicing plane with the scaling line. (a–e) The variable space is sliced by the plane of trading partners k equal to 0–4 in common logarithm. (f–j) The variable space is sliced by the plane of employee number l equal to 0–4. (k–q) The variable space is sliced by the plane of annual sales (in million yen) s equal to 0–6. Yellow solid curves represent the intersection curves of the scaling line with the slice.

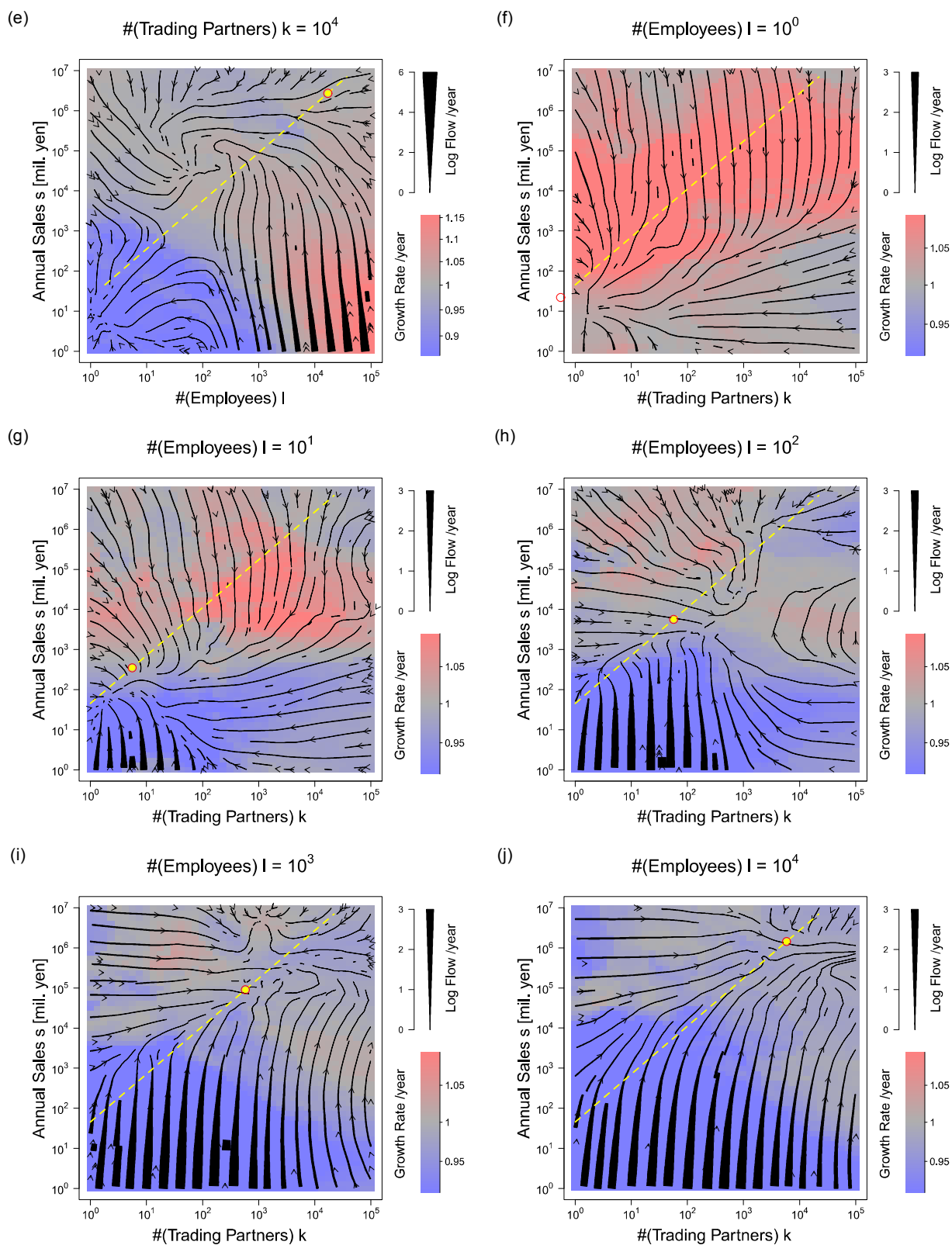


Figure S9—Continued.

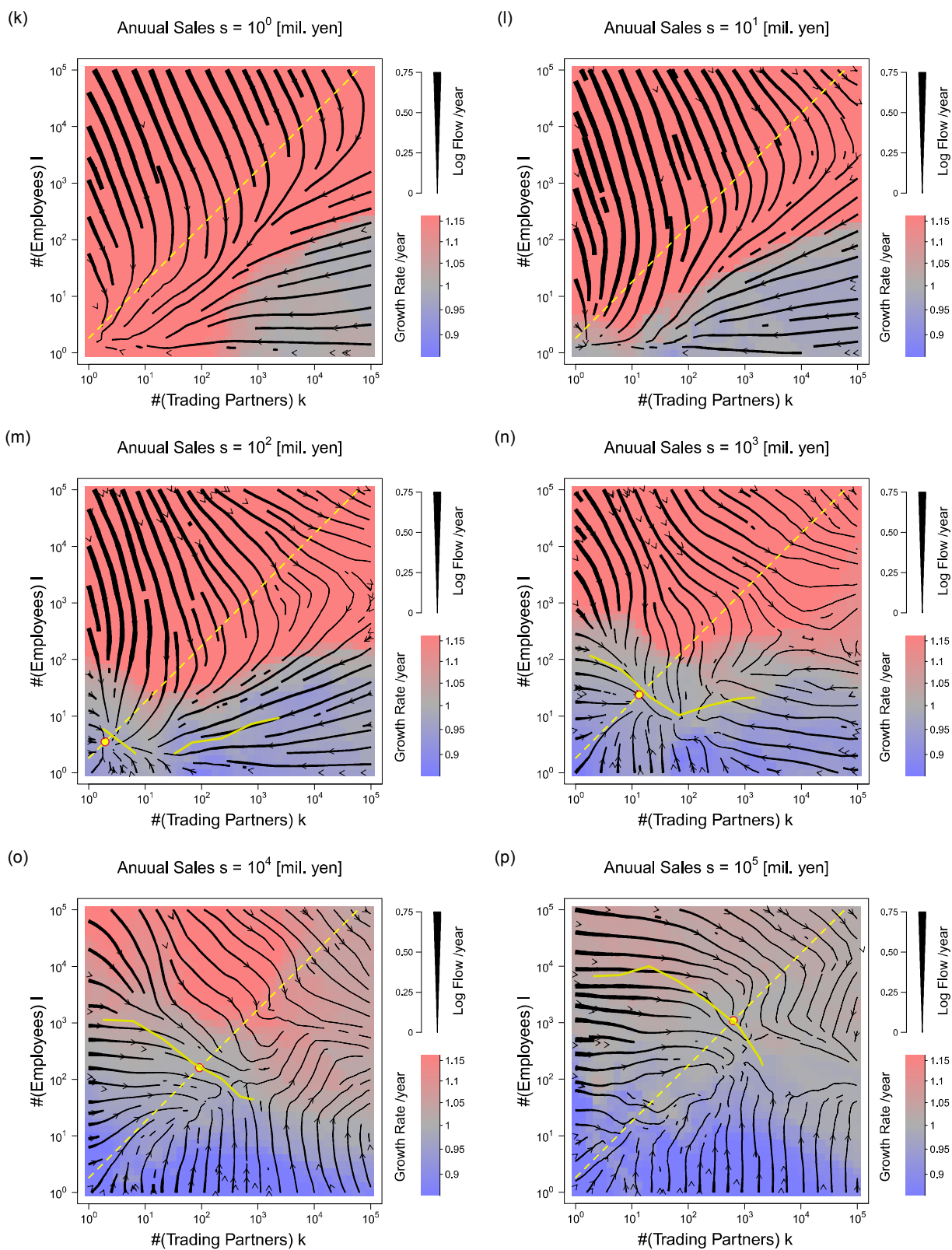


Figure S9—Continued.

(q)

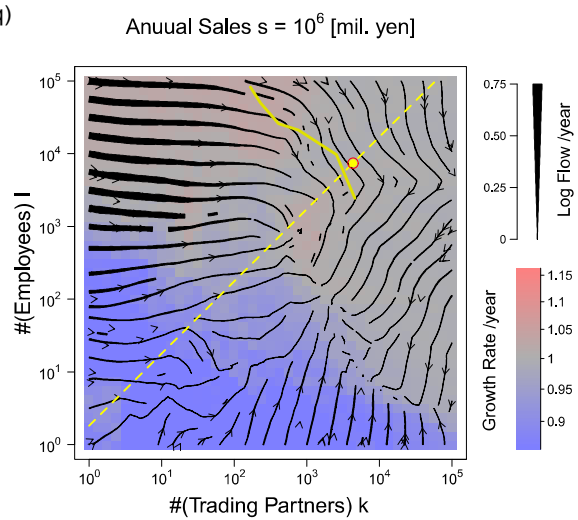


Figure S9—Continued.

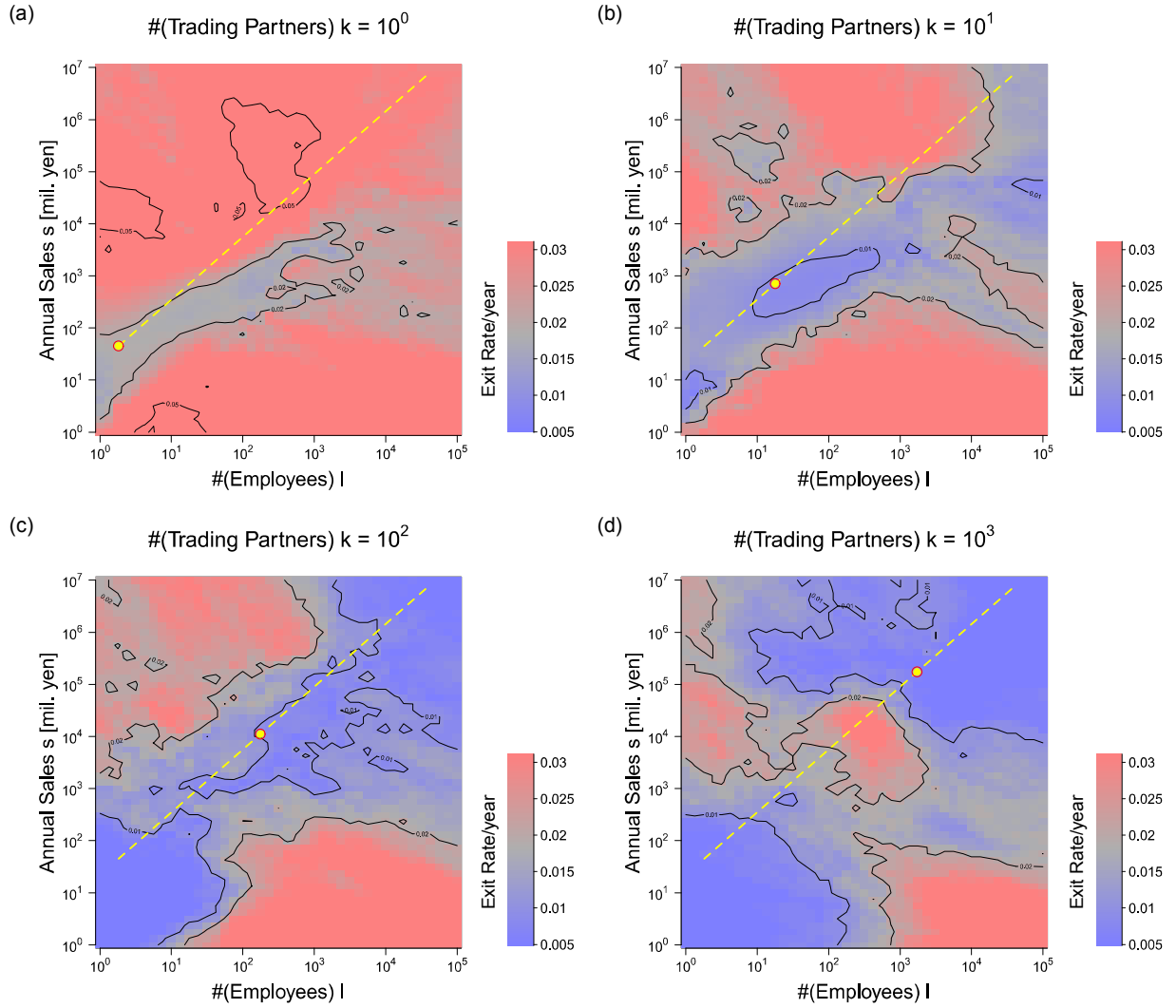


Figure S10. Estimated exit rate per year in the slice of the log-transformed vector space. The estimated average exit rates are illustrated by the background color, with red, grey and blue representing exit rates higher than, equal to and lower than the medium value, respectively. The yellow dashed line indicates the orthogonal projection to the "slicing line" and the yellow and red point on the line represents the intersection point of the plane with the scaling line. We add contours to show clearly the regions where exit rates are high or low. (a–e) The variable space is sliced by the plane of trading partners k equal to 0–4 in common logarithm. (f–j) The variable space is sliced by the plane of employee number l equal to 0–4. (k–q) The variable space is sliced by the plane of annual sales (in million yen) s equal to 0–6. Yellow solid curves represent the intersection curves of the scaling line with the slice.

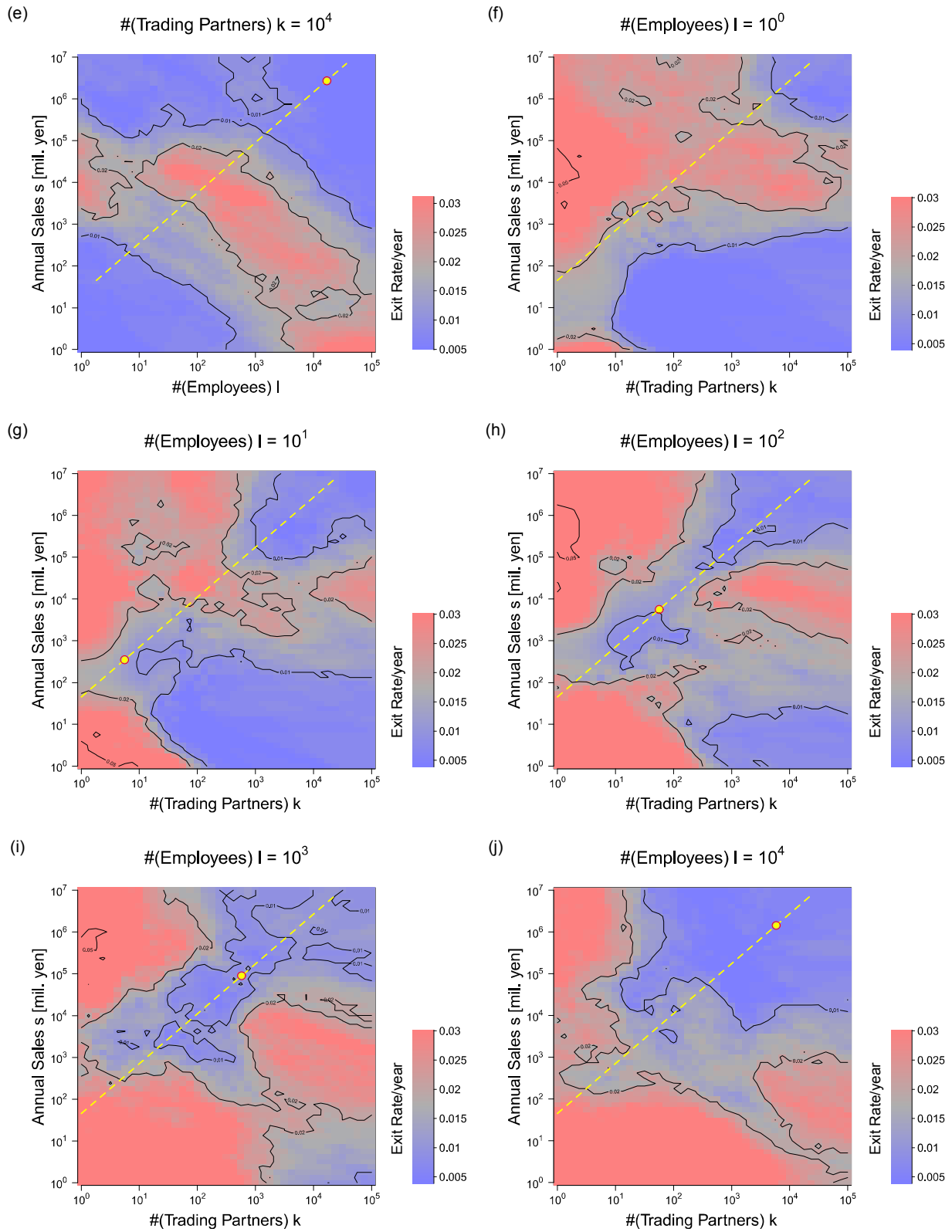
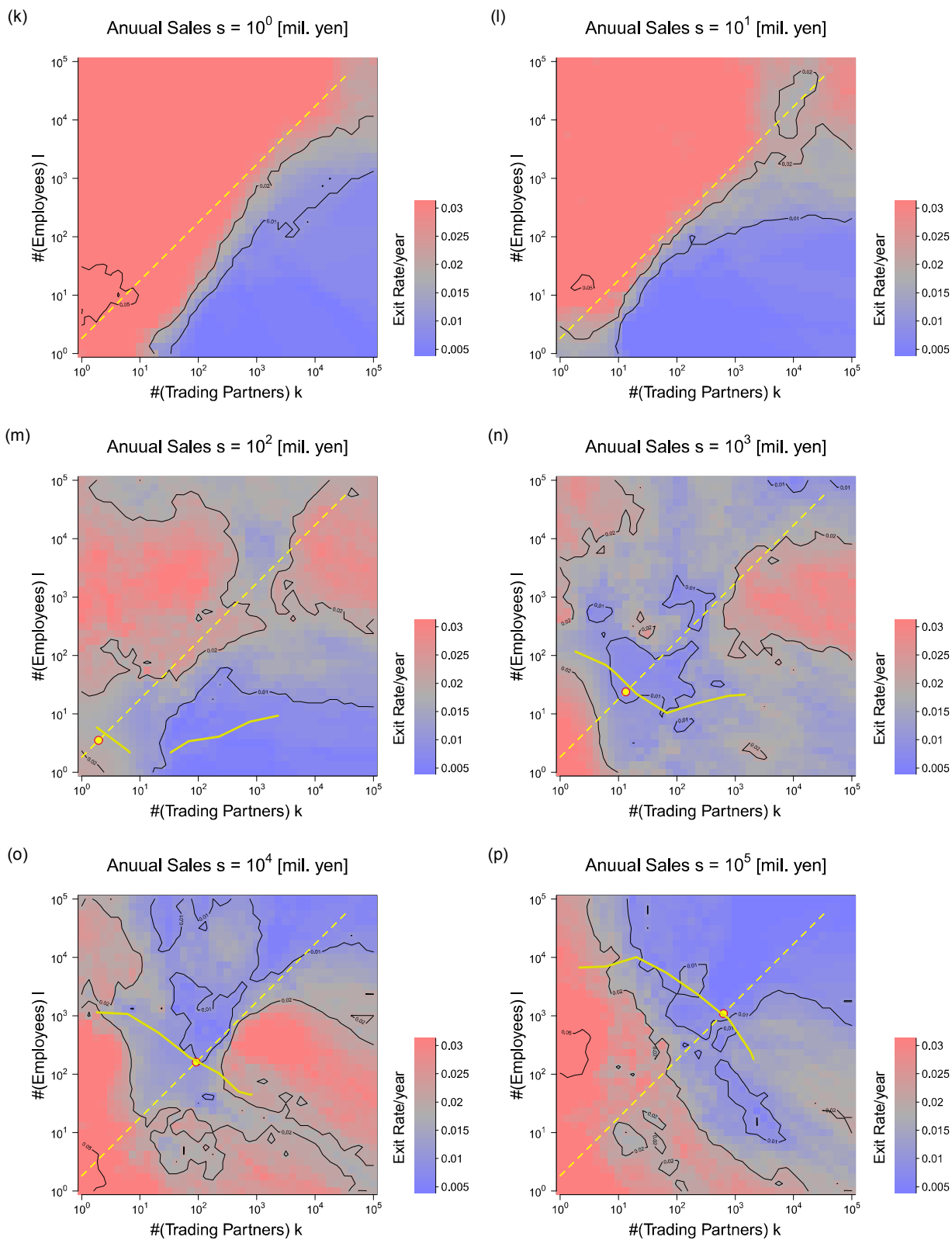


Figure S10—Continued.



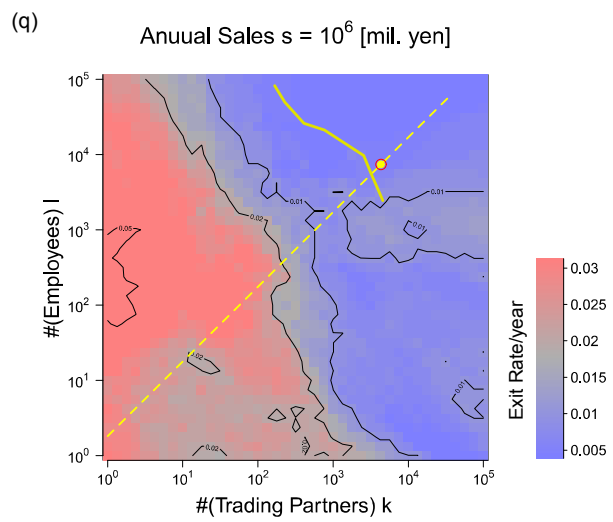


Figure S10—Continued.

Table S1. Descriptive Statistics of the Final Data for Different Years.

Variable	Year	Mean	Standard Deviation	Minimum	25%-quantile	Median	75%-quantile	Maximum	Interquartile Range	Geometric Mean	Geometric Stand. Dev.
Number of Trading Partners	1994	4.740	31.46	1	1	2	4	7,881	3	2.498	2.335
	1995	4.979	32.39	1	1	2	4	8,013	3	2.617	2.359
	1996	5.181	33.03	1	1	3	5	8,009	4	2.722	2.375
	1997	5.395	33.43	1	1	3	5	7,945	4	2.826	2.398
	1998	5.533	33.50	1	2	3	5	7,696	3	2.908	2.403
	1999	5.615	33.21	1	2	3	5	7,393	3	2.961	2.407
	2000	5.727	33.30	1	2	3	5	7,082	3	3.018	2.415
	2001	5.854	33.42	1	2	3	5	6,864	3	3.080	2.429
	2002	5.914	34.12	1	2	3	5	6,424	3	3.100	2.437
	2003	5.968	33.38	1	2	3	5	6,007	3	3.118	2.456
	2004	6.073	33.32	1	2	3	5	5,832	3	3.163	2.472
	2005	6.217	34.38	1	2	3	6	5,562	4	3.225	2.484
	2006	6.345	36.35	1	2	3	6	10,987	4	3.277	2.501
	2007	6.472	38.26	1	2	3	6	14,941	4	3.325	2.519
	2008	6.841	39.84	1	2	3	6	15,587	4	3.474	2.570
	2009	6.936	39.89	1	2	3	7	15,504	5	3.512	2.593
	2010	6.890	39.98	1	2	3	7	15,466	5	3.467	2.608
	2011	6.885	40.17	1	2	3	7	15,252	5	3.456	2.616
	2012	6.898	40.63	1	2	3	7	15,161	5	3.455	2.623
	2013	6.962	41.31	1	2	3	7	14,928	5	3.488	2.627
	2014	7.005	41.15	1	2	3	7	14,895	5	3.501	2.637
	2015	7.058	40.99	1	2	3	7	14,740	5	3.536	2.640

(Continued)

Table S1. Continued.

Variable	Year	Mean	Standard Deviation	Minimum	25%-quantile	Median	75%-quantile	Maximum	Interquartile Range	Geometric Mean	Geometric Stand. Dev.
Number of Employees	1994	31.48	424.1	1	3	7	18	208,028	15	8.184	3.787
	1995	30.86	407.2	1	3	7	18	191,436	15	8.059	3.781
	1996	30.21	396.3	1	3	7	18	186,706	15	7.947	3.763
	1997	29.71	374.0	1	3	7	17	161,488	14	7.830	3.764
	1998	28.97	360.7	1	3	7	17	146,744	14	7.597	3.763
	1999	27.57	316.5	1	3	6	15	77,033	12	7.235	3.743
	2000	26.86	311.1	1	3	6	15	84,242	12	7.010	3.741
	2001	25.85	299.1	1	3	6	15	91,026	12	6.764	3.722
	2002	24.78	287.3	1	3	5	14	97,474	11	6.464	3.705
	2003	24.08	277.4	1	2	5	13	100,090	11	6.253	3.701
	2004	24.18	380.1	1	2	5	13	271,368	11	6.162	3.717
	2005	24.74	382.2	1	2	5	13	261,937	11	6.162	3.766
	2006	24.51	357.4	1	2	5	13	256,572	11	6.130	3.759
	2007	25.15	384.4	1	2	5	13	254,177	11	6.111	3.787
	2008	25.14	335.3	1	2	5	13	143,276	11	6.023	3.791
	2009	24.65	330.7	1	2	5	12	140,846	10	5.842	3.773
	2010	23.80	325.2	1	2	5	12	136,906	10	5.644	3.745
	2011	23.68	323.9	1	2	5	11	139,320	9	5.549	3.740
	2012	24.02	366.7	1	2	5	11	209,000	9	5.501	3.752
	2013	23.89	349.4	1	2	5	11	200,601	9	5.489	3.762
	2014	24.06	354.8	1	2	4	11	194,688	9	5.471	3.772
	2015	24.46	356.7	1	2	5	12	193,934	10	5.516	3.803

(Continued)

Table S1. Continued.

Variable	Year	Mean	Standard Deviation	Minimum	25%-quantile	Median	75%-quantile	Maximum	Interquartile Range	Geometric Mean	Geometric Stand. Dev.
Annual Sales [million yen]	1994	2,379	143,058	1	70	180	480	39,262,034	410	198.6	4.587
	1995	2,356	141,562	1	70	180	469	39,696,346	399	195.1	4.601
	1996	2,369	141,412	1	70	178	470	39,841,681	400	194.2	4.636
	1997	2,377	146,488	1	70	173	464	55,760,824	394	191.3	4.694
	1998	2,239	139,637	1	62	160	426	56,946,664	364	176.1	4.707
	1999	2,059	127,448	1	58	145	390	48,191,575	332	161.3	4.685
	2000	2,024	125,415	1	54	137	370	46,324,909	316	153.2	4.734
	2001	1,967	128,025	1	50	128	350	48,549,384	300	143.5	4.799
	2002	1,971	150,814	1	45	118	321	67,876,272	276	132.3	4.825
	2003	2,015	167,481	1	43	110	309	75,747,636	266	125.9	4.878
	2004	1,988	156,492	1	42	109	304	71,403,288	262	124.0	4.940
	2005	1,996	150,736	1	41	108	306	74,671,935	265	123.8	5.002
	2006	2,157	183,258	1	40	107	308	106,808,600	268	123.0	5.079
	2007	2,214	185,985	1	40	104	305	105,792,700	265	121.3	5.161
	2008	2,294	246,066	1	39	100	300	181,743,800	261	114.7	5.277
	2009	2,163	242,882	1	32	90	260	177,479,800	228	99.07	5.371
	2010	2,140	258,782	1	30	80	237	175,797,700	207	89.95	5.394
	2011	2,168	255,034	1	30	80	230	174,653,200	200	87.06	5.475
	2012	2,149	256,620	1	29	80	230	175,635,300	201	86.11	5.517
	2013	2,173	262,035	1	29	79	224	176,096,136	195	85.21	5.528
	2014	2,371	283,726	1	29	80	231	176,612,700	202	86.70	5.668
	2015	2,405	289,929	1	29	80	235	177,710,700	206	87.06	5.696

†Decimal parts are rounded when the figure exceeds 4 digits.

Supplementary References

- [1] P. Cirillo and J. Hüsler, *Physica A* **388**, 1546 (2009).
- [2] T. Ogwang, *Empir. Econ.* **41**, 473 (2011).
- [3] B. Fix, *PLoS One* **12**, e0171823 (2017).
- [4] M. H. R. Stanley, L. A. N. Amaral, S. V. Buldyrev, S. Havlin, H. Leschhorn, P. Maass, M. A. Salinger, and H. E. Stanley, *Nature* **379**, 804 (1996).
- [5] G. Bottazzi and A. Secchi, *RAND J. Econ.* **37**, 235 (2006).
- [6] H. Watanabe, H. Takayasu, and M. Takayasu, *Physica A* **392**, 741 (2013).
- [7] A. C. Davison and D. V. Hinkley, *Bootstrap Methods and Their Application* (Cambridge University Press, Cambridge, 1997).
- [8] Cabinet Office Government of Japan, (2017).
- [9] Cabinet Office Government of Japan, (2017).
- [10] L. A. N. Amaral, S. V. Buldyrev, S. Havlin, P. Maass, M. A. Salinger, H. Eugene Stanley, and M. H. . Stanley, *Physica A* **244**, 1 (1997).
- [11] G. De Fabritiis, F. Pammolli, and M. Riccaboni, *Physica A* **324**, 38 (2003).
- [12] M. Takayasu, H. Watanabe, and H. Takayasu, *J. Stat. Phys.* **155**, 47 (2014).
- [13] A. Ishikawa, S. Fujimoto, T. Mizuno, and T. Watanabe, in *Proc. Asia-Pacific Econophysics Conf. 2016 — Big Data Anal. Model. Towar. Super Smart Soc.* —, edited by M. Takayasu (Journal of the Physical Society of Japan, Tokyo, 2017), p. 11005.
- [14] G. Turk and D. Banks, in *Proc. 23rd Annu. Conf. Comput. Graph. Interact. Tech. - SIGGRAPH '96* (ACM Press, New York, New York, USA, 1996), pp. 453–460.